

# Identification and Climatology of Cut-off Lows near the Tropopause

R. Nieto,<sup>a,b</sup> M. Sprenger,<sup>c</sup> H. Wernli,<sup>d</sup> R. M. Trigo,<sup>b,e</sup>  
and L. Gimeno<sup>a</sup>

<sup>a</sup>*Universidad de Vigo, Facultad de Ciencias, Ourense, Spain*

<sup>b</sup>*University of Lisbon, CGUL-IDL, Lisbon, Portugal*

<sup>c</sup>*Institute for Atmospheric and Climate Science, ETH Zürich, Zürich, Switzerland*

<sup>d</sup>*Institute for Atmospheric Physics, University of Mainz, Mainz, Germany*

<sup>e</sup>*Universidade Lusófona, Departamento de Engenharias, Lisbon, Portugal*

Cut-off low pressure systems (COLs) are defined as closed lows in the upper troposphere that have become completely detached from the main westerly current. These slow-moving systems often affect the weather conditions at the earth's surface and also work as a mechanism of mass transfer between the stratosphere and the troposphere, playing a significant role in the net flow of tropospheric ozone. In the first part of this work we provide a comprehensive summary of results obtained in previous studies of COLs. Following this, we present three long-term climatologies of COLs. The first two climatologies are based on the conceptual model of a COL, using European Centre for Medium-range Weather Forecasts (ECMWF) analyses (1958–2002) and National Centers for Environmental Prediction–National Center for Atmospheric Research (1948–2006) reanalysis data sets. The third climatology uses a different method of detection, which is based on using potential vorticity as the physical parameter of diagnosis. This approach was applied only to the ECMWF reanalysis data. The final part of the paper is devoted to comparing results obtained by these different climatologies in terms of areas of preferential occurrence, life span, and seasonal cycle. Despite some key differences, the three climatologies agree in terms of the main areas of COL occurrence, namely (1) southwestern Europe, (2) the eastern north Pacific coast, and (3) the north China–Siberian region. However, it is also shown that the detection of these areas of main COL occurrence, as obtained using the potential vorticity approach, depends on the level of isentropic analysis used.

**Key words:** cut-off low pressure systems (COLs); conceptual model; potential vorticity

## Introduction

A cut-off low pressure system (COL) corresponds to a closed low in the upper troposphere that has become completely detached (“cut off”) from the basic westerly current in the jet stream<sup>1,2</sup> and which is usually advected toward the equatorial side of the mid-latitude westerlies.<sup>3</sup> A COL usu-

ally starts its life cycle as a trough in the middle and upper troposphere (Fig. 1). Traditionally, COLs have been recognized as depressions mostly located in mid latitudes, which are characterized by closed geopotential contours in isobaric maps (with a cold core, Fig. 2) that have more or less concentric isotherms around the central core.<sup>1</sup> Because the jet stream corresponds to the boundary between two very different air masses, the air mass trapped within a COL maintains its polar characteristics (i.e., it is colder than the surrounding air). Its intensity is highest in the upper troposphere and the

Address for correspondence: Raquel Nieto, Edificio de Física, Campus Universitario de Ourense–Universidade de Vigo, As Lagoas s/n, 32004 Ourense, Spain. rnieto@uvigo.es

## TYPICAL SCHEME OF COL DEVELOPMENT

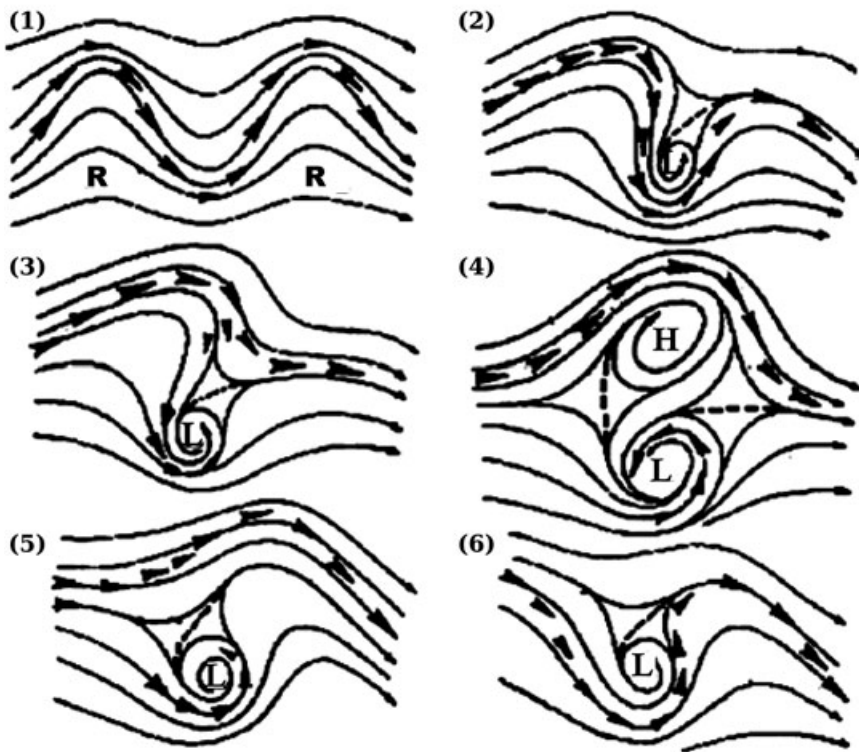


**Figure 1.** Process of isolation and evolution of a COL. (1) Undulation of the meridional circulation in the jet stream (arrows). Ridges are denoted by R. (2) Southerly north–south elongation. L indicates the COL during its initial stages. (3) Initial isolation or strangulation. (4) Total isolation. The COL has become completely detached from the originating circulation and has developed its own circulation. A ridge or region of high pressures often develops on its northerly part, H in the figure. (5) Start of absorption. (6) South–north elongation and complete absorption

magnitude of the associated cyclonic circulation decreases toward the earth's surface, being even possible to find anticyclonic circulation at the surface.<sup>4</sup>

COLs can also be recognized as maxima of potential vorticity (PV) on isentropic surfaces.<sup>5,6</sup> It is well known that bands of strong PV gradients coincide with the jet streams and act as wave guides for Rossby wave propagation.<sup>7</sup> Rossby wave breaking in the upper troposphere (near the tropopause) can lead to pronounced excursions of stratospheric air southward and, eventually, to the formation of COLs.<sup>8</sup> The genesis of these systems in mid latitudes can be seen as the displacement of a region of high PV from its polar reservoir, leading to

the detachment of a discrete cut-off area. PV may, therefore, be regarded as another useful quantity for the identification of cut-off lows (Fig. 3).

Irrespective of the method of identification, COLs can be associated with intense stratosphere–troposphere exchange (STE) (Refs. 8–11 and references therein). In fact, STE associated with COLs has been recognized as being responsible, at least to a certain extent, for the appearance of anomalously high values of tropospheric ozone in northern mid latitudes<sup>12,13</sup> and subtropical areas.<sup>14,15</sup> In COLs, the tropopause is anomalously low and might be characterized by steep structures and folds. It is proposed that STE in these systems



**Figure 2.** Image of a COL at 18 UTC on 10 October 2001 in an isobaric map at the 500 hPa level. Solid lines show the geopotential (m) and dashed lines show the temperature ( $^{\circ}\text{C}$ ). The isolated COL is over the SW Iberian peninsula. The background image is from the Meteosat infrared (IR) channel. (Figure from the INM, National Meteorology Institute of Spain.)

occurs mainly from condensational or radiative erosion of the tropopause (e.g., Refs. 16, 17). In addition, turbulent three-dimensional mixing near the jet stream associated with the COL and tropopause folding along the system<sup>5,18</sup> can be considered as another possible mechanism leading to STE. Separation of air from the general flow into a COL is typically associated with an intense STE,<sup>19</sup> and, during the later phase of a COL life cycle, filamentation of the outer layers<sup>20</sup> can be responsible for additional very effective STE.

Once COLs are disconnected from the environmental zonal flow, the jet stream no longer controls the motion of the isolated system and its motion becomes more erratic and difficult to predict. The COL may remain stationary and spin for days or, on other occasions, it may move westward in the opposite direction to the prevailing flow (i.e., retrogression). The move-

ment of a COL is usually slow, and it remains over a region until it reconnects with the polar reservoir or until it weakens and eventually dissipates. These systems are, therefore, capable of considerably affecting weather conditions at the earth's surface, for periods of several days at a time (Ref. 2 and references therein).

As a general rule, the troposphere below the COL is unstable and severe convective events can occur, depending on surface conditions. However, COLs produce significant precipitation only when the air mass below the COL is significantly moist and becomes potentially unstable.<sup>21</sup> This instability occurs quite frequently below COLs in the southern mid latitudes (i.e., near  $30\text{--}40^{\circ}\text{N}$ ), and convective events can occur, sometimes severely, in the affected areas.

Because of their erratic movement, their self development and occasionally their dissipative characteristics, and the thermodynamic

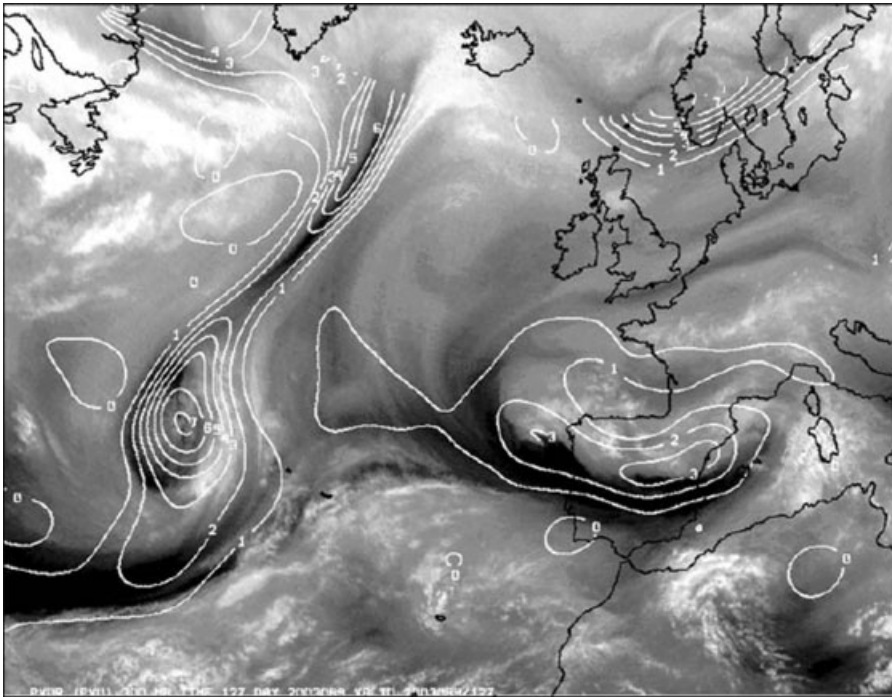


**Figure 3.** COL detected over the North Atlantic Ocean according to the potential vorticity field (PV;  $1 \text{ PVU} = 1 \times 10^{-6} \text{ m}^2 \text{ s}^{-1} \text{ K kg}^{-1}$ ) at 300 hPa, based on a HIRLAM model on 30 March 2003 at 12 UTC. Image of the water vapor background for the same time from the Meteosat satellite. A long thin strand links the COL with the PV-rich source or production region from which it became detached. Image from the INM (National Meteorology Institute of Spain).

instability frequently associated with these features, weather forecasting for systems that are affected by COLs is particularly difficult. COLs are associated with many substantial forecasting problems, mainly from the different characteristics of the underlying terrain and to the presence/absence of a warm ocean that permits/inhibits convection.<sup>21</sup> Thus, prediction of the distribution of precipitation associated with COLs presents a considerable challenge, especially when the precipitation is from enhanced convection over a warm sea. When moisture is available, COLs can trigger multiple bands of clouds, and these can bring moderate to heavy rainfall over large areas. In particular, they are among the most severe weather systems that affect southern Europe and northern Africa and are responsible for some of the most catas-

trophic weather events in terms of precipitation rate.<sup>22–25</sup>

The main objectives of this paper are twofold: (1) to provide a review of the COL concept and its relevance for weather and climate in several regions and (2) to present an update of two, more recent, comprehensive, hemispheric climatologies of COLs.<sup>6,26</sup> The remainder of the paper is organized as follows. Section 2 defines the synoptic conceptual model of COLs and their physical parameters. In Section 3, a review of previous climatologies using subjective and objective methods is presented. In Section 4, we present updated COL data sets for National Centers for Environmental Prediction–National Center for Atmospheric Research (NCAR–NCEP) and ERA-40 reanalyses, using the objective method of Nieto

*et al.*,<sup>26</sup> and for ERA-40 reanalyses, using the method of Wernli and Sprenger.<sup>6</sup> In Section 5, we present a comparison of these climatologies and our conclusions.

## Conceptual Model of a Cut-off Low

A conceptual model is a visual representation of the essential features of a meteorological phenomenon, including the principal processes that are associated with it. A complete conceptual model provides: (a) a definition of the phenomenon in terms of features recognizable by observations, analysis, or validated simulations; (b) a description of its life cycle in terms of its appearance, size, intensity, and accompanying weather patterns; (c) a statement of the controlling physical processes, which enables an understanding of the factors that determine the mode and rate of evolution of the phenomenon; (d) a specification of the key meteorological fields that demonstrate the main processes; and (e) guidance for predicted meteorological conditions or situations using the diagnostic and prognostic fields that best discriminate between development or nondevelopment, in addition to guidance that may be used for predicting displacement and evolution.<sup>2</sup>

Conceptual models are useful because they provide meteorologists with a tool for both understanding and diagnosing observed phenomena. For both forecasters and modellers, they provide tools for diagnosing the output of numerical models and for identifying errors in numerical forecast models.<sup>2</sup>

Some details of the meteorological properties of COLs can be found in the meteorological literature that describes case studies (e.g., Refs. 27, 28) and in more general studies about upper-level flow structures (e.g., Refs. 1, 29), but a complete description of the conceptual model of COLs was developed under the COST initiative (European Cooperation in the Field of Scientific and Technical Research) Action 78 entitled "Implementation of an European Re-

search Action on the Development of Nowcasting Techniques."<sup>2</sup>

The usual conceptual model of a COL<sup>2</sup> describes this system as a nonfrontal synoptic-scale phenomenon with a typical life cycle that is separated into four stages: upper-level trough, tear off, cut off, and final stage, as described below. This section also provides information about cloud structure during the different phases of the COL life cycle, the associated horizontal and vertical meteorological characteristics, and, finally, weather events associated with COLs.

## Meteorological Background

The schematic COL life cycle in terms of its meteorological structure is shown in Figure 4, with Figure 5 showing the evolution of a real COL during January 1998 over central Europe. These two figures provide an insight into the four stages of the COL life cycle:

- (1) The upper-level trough: An essential condition for COL development is the existence of an amplifying synoptic-scale wave in the upper layers of the troposphere. The temperature wave situated behind the geopotential wave advects substantial amounts of cold air into the upper-level trough and warm air to the ridge. It is also a requirement that the vertical axis of the trough tilts backward with elevation (Fig. 6). If these conditions occur simultaneously, the geopotential and temperature waves are amplified. Typically, this amplification is also accompanied by a decrease of the zonal wavelength. The isohyses and isotherms show a shift toward the equator, which leads to a deepening of the trough.
- (2) The tear-off stage: In this stage, the shape of the geopotential contour assumes an inverted omega form. The increase in the amplitude of the waves continues, the trough deepens, and it starts to detach from the meridional stream. The cold air

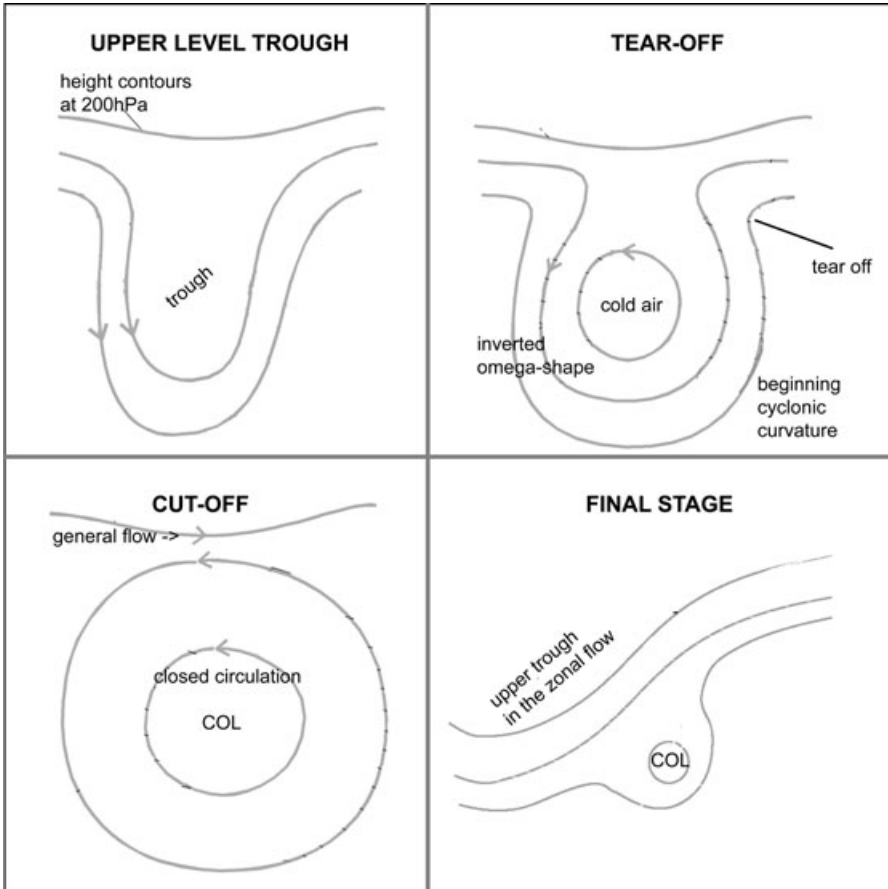


**Figure 4.** Diagram of the typical synoptic situation of a cut-off low showing the different stages of its life cycle using the geopotential field at 200 hPa.

streaming toward the equator is cut off from the general polar flow, and the warm air flowing toward the pole is cut off from the general subtropical flow. At the end of this process, a cold-core, upper-level, low-pressure system is formed within the southern part of the trough.

- (3) The cut-off stage: This stage begins when the tear-off process is finished and the upper-level low becomes more pronounced. The wind field at the uppermost tropospheric levels acquires a well-developed closed circulation, often completely cut off from the general zonal flow. This circulation is strongest near 200 hPa but typically penetrates down

to the mid troposphere (500 hPa) and, in some cases, even to the earth's surface. The maintenance of the COL, and therefore its life span, depends on various factors, in particular on thermodynamic stability below the COL.

- (4) The final stage: The main factor leading to the dissolution of a COL is convection. If the thermodynamic stability below the COL is sufficiently reduced, convection and associated cloud diabatic effects can lead to a decay of the COL (and strong associated STE as described in Section 1) within a few days. This effect is more efficient over warm surfaces (and in the presence of a significant vertical

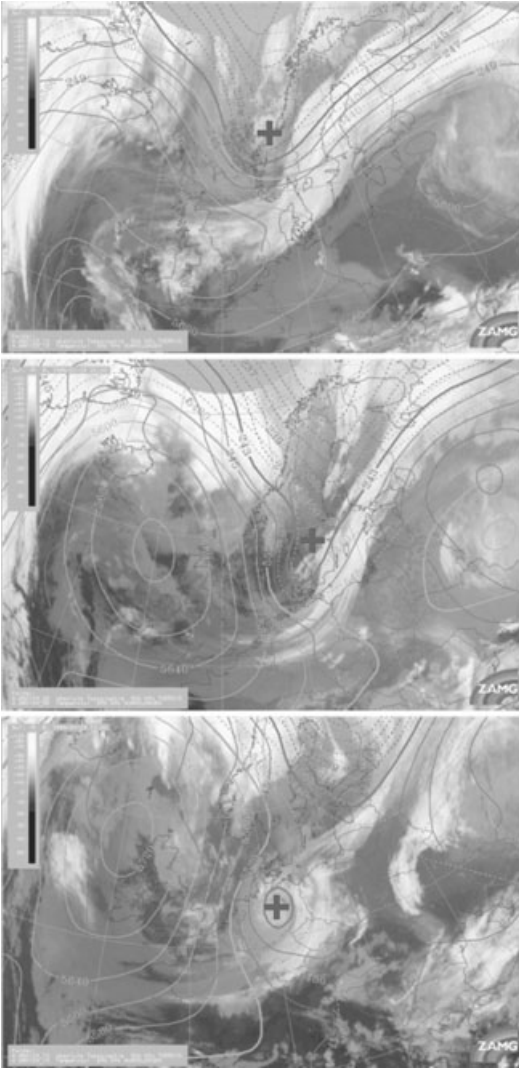


**Figure 5.** Cut-off low system detected over Europe (indicated with a cross) showing the different stages of its life cycle. Top panel: upper-level trough detected on 23 January 1998 at 12 UTC; Middle: tear off detected on 24 January 1998 at 00 UTC and Bottom: cut-off stage detected on 24 January 1998 at 12 UTC. Images of the infrared (IR) background for the same time from the Meteosat satellite showing the cloud cover. Height contours at 500 hPa are continuous lines and temperature field (in K) at 500 hPa is denoted by dotted lines. (Figures adapted from Zentrale Anstalt für Meteorologie und Geodynamik of Austria (ZAMG).)

temperature gradient), while over cold surfaces the COL will not dissolve until it is either caught by the main stream and merges with a large upper-level trough in

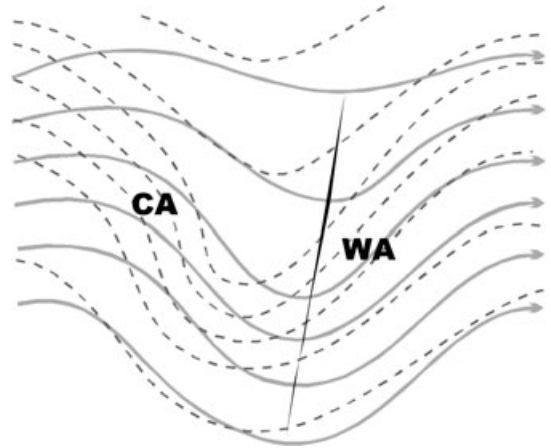


**Figure 6.** Temperature wave (dashed lines) and potential wave (solid lines). The vertical axis of the trough is denoted by the solid black line. The temperature field shows cold advection (CA) in the area of the geopotential trough and warm advection (WA) at the ridge of the wave. (Figures adapted from ZAMG.)

the main zonal flow or it drifts over a warm surface. About 15% of COLs are caught by the main flow.<sup>2</sup> A COL typically lasts for about 2–5 days before being destroyed by diabatic heating.<sup>5,16</sup>

### Cloudiness Structure

COLs have a very well-defined complex cloud structure and are easily detected in satellite imagery on different channels: infrared (IR), visible (VIS), and water vapor (WV). The degree of cloud cover in COLs depends greatly on the stage of its life cycle, but a higher percentage of cloud cover is always present in the frontal zone because of higher concentrations of high clouds and deep convective clouds. The frontal zone is also characterized as being more active, with cloud-top temperatures of high- and deep-convective cloud lower than in the zone behind it.<sup>30</sup>

A schematic of each cloudiness stage of the COL life cycle is shown in Figure 7 for the IR and WV channels.<sup>2</sup> In Figure 8, images from the WV Meteosat channel show another real COL event. They are described for the four stages of the life cycle<sup>2,30</sup>:

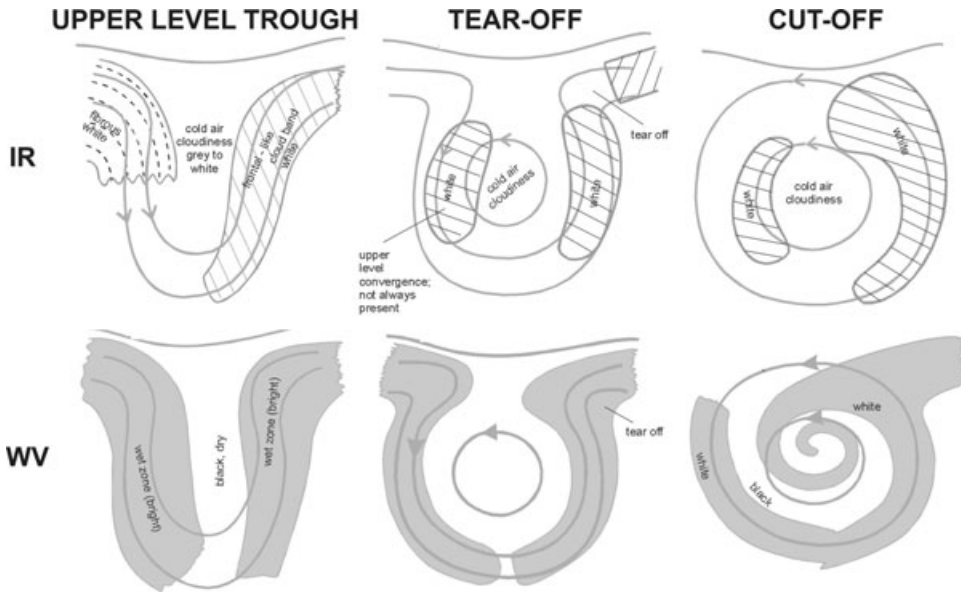


**Figure 7.** Diagram of the typical synoptic situation of a cut-off low showing the different stages of its life cycle using the geopotential field and the satellite images (overlapped dashed areas for IR channel and shaded areas for WV channel). (Figures adapted from ZAMG.)

- (1) The upper-level trough stage is characterized by a well-developed frontal cloud band. This band appears as white in VIS and IR images, indicating the high thickness and the multiple layers of clouds. Some fibrous and rough high cloudiness appears behind the upper-level trough,<sup>30</sup> which is normally associated with a warm front. This cloudiness is in the upper troposphere, so it is possible to detect it only in IR and WV images. These two bands appear as light gray bands of water vapor (wet areas) in WV images, and the core of the COL appears in black because of the dry air that characterizes the area around the trough axis. In the center of the trough there is also cold air cloudiness that can only be detected in IR and VIS images. Usually about 50% of the COL area is covered by some type of cloud, with a larger percentage in the frontal region.
- (2) In the tear-off stage, the cloudiness is caused predominantly by convergence. The frontal cloud band becomes broken where the isolines fold (in the far north-

east part of the trough). The southern part of this cloud band starts to curve cyclonically. In some cases, this cyclonic process also occurs in the rearward fibrous cloud band. The differences in cloudiness between the two zones increase as a result of deep convection in the frontal zone. IR images show white tones from light gray to white and VIS images show the cloud bands in dark gray to gray, restricted to the area of the tear off. WV images show a notable cyclonic band of water vapor extended over the entire trough, indicating the moisture sources. At this stage, the center of the COL becomes dominated by dark gray zones, indicating the existence of dry (at upper-level stratospheric) air.

- (3) In the cut-off stage, a cyclonic spiral of moisture appears in WV images starting from the edge of the COL core. This stage is characterized by a more uniform distribution of cloudiness, with IR imagery showing two white cloud bands ahead of and to the rear of the trough. At the same time, convection within the core of the

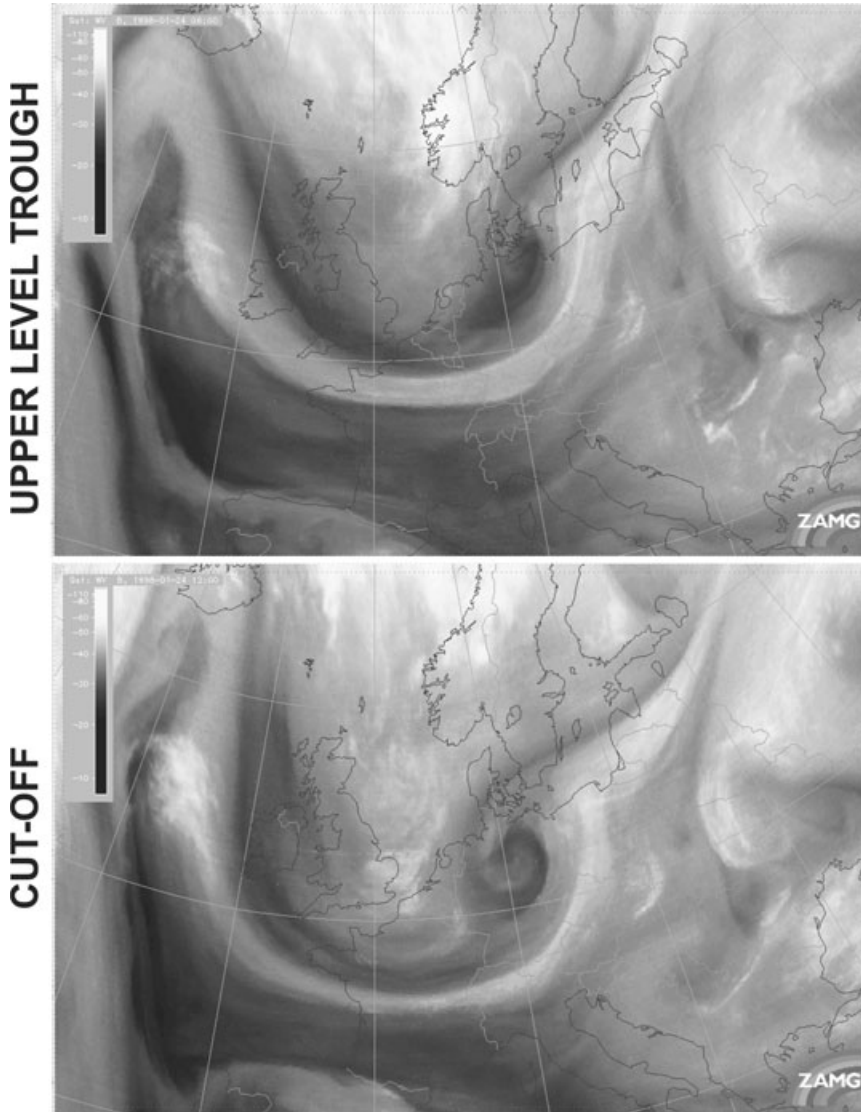


**Figure 8.** Cut-off low detected on water vapor images (WV) from Meteosat during the upper-level trough and cut-off stages on 24 January 1998 at 06 UTC and 12 UTC, respectively (Images from ZAMG.)

COL is possible because of reduced stratification beneath the COL. High and deep convection clouds appear in the center of the COL, although with differing intensity and structure depending on whether the COL is continental or oceanic. Over land the convective cells are detected as being embedded in a continuous mantle of lower cloud, while over relatively warm ocean waters the core convection is very intense and the cells appear isolated.

- (4) In the final stage when the COL life cycle ends, it is possible to detect in IR images that the cloudiness of the COL merges with the developed and structured cloud band (white color) that is associated with the main zonal flow.

A general characteristic throughout the entire life span of a COL is that in the frontal zone the percentage of very bright IR pixels is higher than in the rearward zone (70% versus

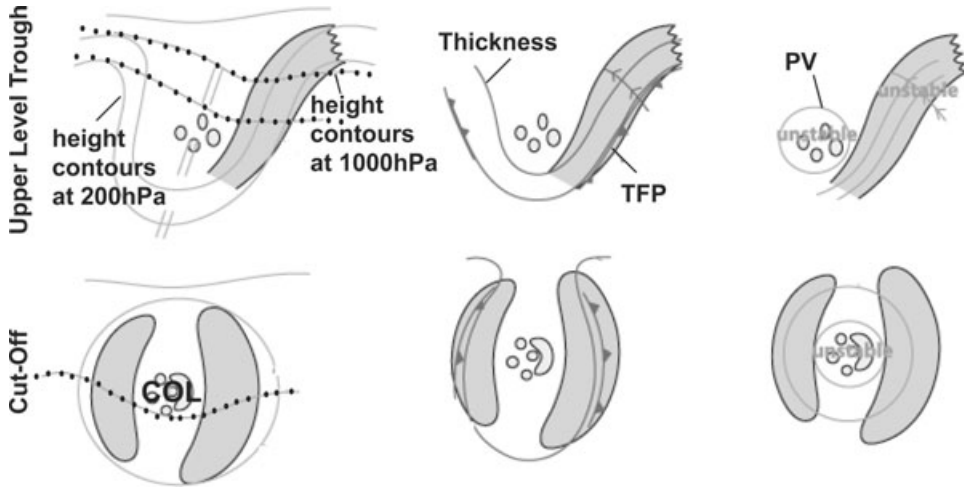


**Figure 9.** Diagram of the typical synoptic situation of a cut-off low showing the upper-level trough and cut-off stages of its life cycle using the geopotential fields at 200 hPa and 1000 hPa (left), the equivalent thickness and TFP scheme (middle), and the PV scheme (right). The cloud cover is overlapped by shaded areas. (Figures adapted from ZAMG.)

30%), because of the contribution of cloudiness associated with convective systems. This feature is particularly evident for the first stage over the northern part of the frontal cloud band. Moreover, the difference between the rearward and frontal zones seems to be accentuated for COLs during the cold season.

### Horizontal Physical Parameters

The meteorological characteristics discussed so far are also associated with some of the principal parameters in horizontal charts, for example, the geopotential field at multiple levels (from the earth surface to the upper troposphere), the equivalent thickness, the thermal front parameter (TFP), and the potential vorticity (PV). These are each considered in turn.

(i) It is useful to consider three geopotential heights in relation to the structure of COLs, namely 200, 500, and 1000 hPa. As previously mentioned, during the initial stage the absolute topography at 200 hPa shows an upper-level trough. Geopotential height contours at the 500 hPa level exhibit the same behavior. During the later stages of de-

velopment, these contours tend to form an inverse omega shape that leads to a closed cyclonic circulation (Fig. 9). However, at 1000 hPa, sometimes no distinct low-level features can be observed at all. The gradient of the geopotential height contours is generally weak at this level. Some weak cyclonic circulation may appear, initiated by the circulation from aloft, during the later phases of a COL.

(ii) Equivalent thickness is the thickness of the atmospheric layer between two pressure surfaces and is often used to locate fronts.<sup>31,32</sup> In a low, this feature is characterized by a thickness ridge in front of the low and a trough or a distinct minimum behind or in the center of the low. The equivalent thickness is given by:  $Z_T^* = -\frac{g}{R} \sum_{lev1}^{lev2} \bar{T}_e \ln\left(\frac{P_u}{P_l}\right)$ , where  $g$  is the acceleration from gravity,  $R$  is the universal gas constant,  $\bar{T}_e$  is the layer mean equivalent temperature,  $P_u$  is the pressure at the top of the layer, and  $P_l$  is the pressure at the bottom of the layer.

(iii) COLs are characterized by two baroclinic zones, one in front of the low, which is connected with a front-like cloud band, and another one behind the low, connected with a

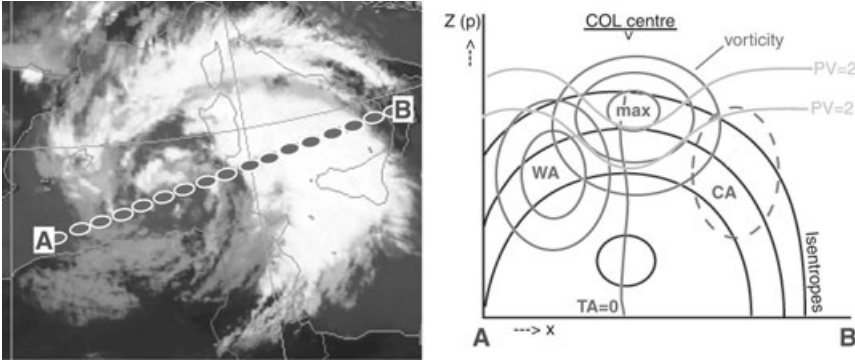


**Figure 10.** Left image shows the vertical cross-section line (A to B) chosen for a cut-off low over the Mediterranean Sea. Right image shows the typical parameters. (Figures adapted from ZAMG.)

baroclinic boundary.<sup>33</sup> There is a clear relationship between the well-known basic definition of a front and the TFP.<sup>34</sup> The TFP is a scalar variable. At its maximum, it fixes the position of the cold front where the temperature begins to fall and the position of the warm front where the temperature stops rising.<sup>35</sup> The mathematical definition of the TFP is:  $TFP = -\nabla |\nabla T| \cdot (\nabla T / |\nabla T|)$ , where  $T$  is the temperature of the analyzed level. The temperature used in the TFP can be taken at any level. The first term of the equation ( $-\nabla |\nabla T|$ ) indicates the change of the temperature gradient and the second one ( $\nabla T / |\nabla T|$ ) the projection in the direction of the temperature gradient. In other words, TFP is the change of temperature gradient in the direction of the temperature gradient. The typical fields of equivalent thickness and TFP in a cut-off low are shown in Figure 9.

- (iv) It is instructive to view COLs in terms of PV on isentropic surfaces.<sup>5</sup> The cut-off process of cold polar air is manifested as a cut off of high-PV stratospheric air masses, and thus COLs can easily be identified as isolated features with stratospheric PV ( $PV > 2$  PVU;  $1 \text{ PVU} = 10^{-6} \text{ K kg}^{-1} \text{ m}^2 \text{ s}^{-1}$ ) on isentropic surfaces.<sup>6</sup> COLs are associated with low tropopause height compared to the surrounding regions (i.e., the tropopause is generally lowest where the isentropic PV is maximum).

### Vertical Structure

In order to have a complete description of the conceptual model of a COL, it is also necessary to describe its vertical structure. Vertical cross sections of (equivalent) potential temperature show cold air in or near the center of the COL and a ridging of the isentropes below the COL. In some cases, equivalent potential temperature even decreases with height in the lowest part of the troposphere, indicating thermodynamic instability. Relative vorticity shows a maximum that is coincident with the ridge structure of the isentropes. This vorticity maximum reflects the strong circulation around the center of the COL. Given that the air within a COL is colder than its surroundings, translations and rotation produce a distinct cold advection (CA) ahead of the COL and warm advection behind it. As noted above, the center of the COL is characterized by a PV maximum. Therefore, in a vertical cross section, higher values of PV are found within a COL than in its surroundings. Some of these parameters are shown in the vertical cross section in Figure 10. Typically, the region with high positive PV values in the upper part of the COL is also characterized by (very) low water vapor content.

### Weather Events

The occurrence of COLs is often connected with severe weather conditions. Convection is

a key factor that determines the distribution of precipitation that is associated with a COL event. Generally, the frontal cloud band at the leading edge of a COL is thick enough to produce precipitation and, in some cases, frontal cloudiness at the rear edge.<sup>2</sup> In general, COLs produce significant precipitation only when they receive a significant transport of moisture at low and mid levels. In these cases, they become potentially unstable air masses.<sup>21</sup> Different rainfall patterns may be expected, depending on the type of terrain below the low system. When a COL occurs over land, its center is usually covered by a low cloud layer, suppressing the condition for convective precipitation. Over warm ocean regions, COLs can be associated with deep convection and intense precipitation. However, the generalized idea that most COLs produce intense convective rainfall has been shown to be misleading in some studies.<sup>25,36</sup> The severity of the storm depends on surface conditions, particularly those related to moisture input. If the conditions are favorable, COLs can produce moderate to heavy rainfall over large areas. Studies over the Mediterranean region (where the occurrence of COLs is common<sup>26</sup>), show that the peak intensity of cyclonic-related precipitation is located at 300–400 km from the COL center.<sup>25,37</sup> Convective rainfall occurs within a radius of about 300 km of the COL center, with a pronounced peak close to the COL center that is displaced marginally eastward, in front of the COL. The region of convective precipitation coincides with an area of reduced stability and with the leading baroclinic area.<sup>2,4</sup> At the same time, large-scale precipitation is distributed along the east–west axis that passes through the COL. In about 50% of cases, it is this precipitation that dominates. It has also been shown that nearly 25–30% of COLs (mainly during autumn) do not induce any type of rainfall<sup>36</sup> and only 25% are dominated by convection. The intensity of the COL can also influence the precipitation type. Shallow COLs tend to produce convective precipitation very close to the low core, with the

probability of precipitation in these cases being relatively low. Moderate precipitation is more common in cases of deep COLs and when the COLs have a large vertical extension in terms of PV. The interaction of the medium- and high-level flows of a COL with the orography and surrounding areas can be another important factor. The orography (changing from the sea surface to the coast and littoral mountains) alters the flow in lower layers, creating the conditions for the development and organization of convective systems.

## Previous Analysis and Climatology of COLs

In recent years, COLs have been studied in some detail, the focus of attention being either the numerical modeling of case studies,<sup>39–43</sup> the impact of COLs on tropospheric ozone,<sup>44–48</sup> mesoscale analysis of the decay of a COL,<sup>20,49</sup> or observations of the associated synoptic weather.<sup>45,50</sup> Fewer climatological studies of COLs also exist that use a variety of methods to identify individual COLs, usually employing different time periods, and that have been developed to characterize limited geographical domains. The approaches also differ in the procedure used to identify the systems, with some of them using subjective analysis (e.g., Refs. 51,52) while others rely on the use of an objective (automated) analysis. These objective approaches can be based on the analysis of geopotential height on a pressure surface (e.g., Refs. 53–55), of PV data (e.g., Refs. 6, 14, 56), or on the physical parameters of the conceptual model of COL.<sup>26</sup> A review of previous climatologies using different methods is presented in the following section and in Table 1.

### Subjective Analysis

Price and Vaughan<sup>51</sup> and Kentarchos and Davies<sup>52</sup> (hereafter PV92 and KD98, respectively) developed similar subjective climatological analyses of COLs over the entire Northern Hemisphere. These subjective studies are

**TABLE 1.** Main Characteristics of Major Studies on COL Climatologies, Showing the Different Periods of Study, Methodology Used, Period of Analysis and Areas Covered

Reference	Approach	Period	Region	Methodology
Parker <i>et al.</i> (1989) <sup>53</sup>	Objective	1950–1985	Northern Hemisphere (24°–82°N)	Geopotential minimum at 500 hPa
Bell & Bosart (1989) <sup>54</sup>	Objective	1963–1985	Northern Hemisphere (20°–70°N)	Geopotential minimum at 500 hPa
Price & Vaughan (1992) <sup>51</sup>	Subjective	1985–1989	Northern Hemisphere (0°–70°N)	Geopotential charts at 200 hPa
		1.10.1982–30.9.1983		
		1990–1994	Northern Hemisphere (0°–70°N)	Geopotential charts at 200 hPa
Kentarchos & Davics (1998) <sup>52</sup>	Subjective			
Hernández (1999) <sup>56</sup>	Objective	1989–1999	Northern Atlantic	Closed contours of PV
Qj <i>et al.</i> (1999) <sup>57</sup>	Subjective	1983–1996	Southern Australia (25°–40°S/110°–150°E)	Geopotential charts at 200 and 500 hPa
Pizarro & Montecinos (2000) <sup>62</sup>	Objective	1979–1996	Coast of Chile (30°–35°S, 80°–75°W and 35°–40°S, 80°–75°W)	Meridional geopotential gradient at 500 hPa
Smith <i>et al.</i> (2002) <sup>58</sup>	Objective	1953–1999	Northern Hemisphere and NE USA	Geopotential minimum at 500 hPa
Novak <i>et al.</i> (2002) <sup>55</sup>	Objective	1953–1999 May–September	Northern Hemisphere and NE USA	Geopotential minimum at 500 hPa
Cuevas & Rodríguez (2002) <sup>14</sup>	Objective	1989–January 1999	Northern Atlantic (60°W–80°N/30°E–20°N)	Closed contours of PV
Nieto <i>et al.</i> (2005) <sup>26</sup>	Objective	1958–1998	Northern Atlantic (20°–70°N)	Conceptual model of COL
Porcú <i>et al.</i> (2007) <sup>25</sup>	Objective-Subjective	1992–2001	Europe (30°W–45°E/20°–60°N)	Conceptual model of COLs and Geopotential charts at 200 hPa
Fuenzalida <i>et al.</i> (2005) <sup>61</sup>	Objective-Subjective	1969–1999	Southern Hemisphere (10°–60°S)	Geopotential minimum and tracks at 500 hPa
Campatella & Possia (2007) <sup>63</sup>	Objective	1979–1988	southern South America (100°–20°W/15°–50°S)	Conceptual model of COL
Wernli & Sprenger (2007) <sup>6</sup>	Objective	1979–1993	Northern Hemisphere	Closed contours of PV

generally only used for relatively short time periods as their approaches are labor intensive. In particular, PV92 was developed for a 1-year period (October 1982 to September 1983) and KD98 for a 5-year period (1990–1994). The authors looked for a closed cyclonic geopotential contour or any closed circulation in the wind vectors at the 200 hPa pressure level. Three types of COL were defined by PV92, namely: a) polar vortex, b) polar, and c) subtropical. Polar COLs, which usually extend to mid-latitude regions, were the most intensely studied systems. According to the study, subtropical COLs are smaller than the other two types and their life span is shorter. The authors concluded that, a priori, subtropical COLs do not play a significant role in the tropospheric ozone budget. They also identified six favored geographic regions for the occurrence of COLs: Europe (the most favored region with 33% of the total number), northern China–Siberia, the north Pacific, northeastern United States and eastern Canada, western United States, and the northeast Atlantic. Analysis of the annual cycle revealed that COLs occurred more often in summer than in winter, particularly in June and July (30% reported by PV92 and 37% by KD98). The season with the least number of COLs was clearly winter (9% in PV92 and 15% in KD98). According to PV92, the seasonal distribution of COLs showed very similar patterns when the analysis was performed separately for the three types of cut-off low. Furthermore, KD98 confirmed the same basic annual cycles for COLs below lat 40°N (subtropical COLs) and for COLs at higher latitudes, between 40° and 70°N (polar COLs). These authors suggested that the seasonal variations in latitudinal temperature gradients and temperature differences between continental and oceanic regions may be responsible for the seasonal cycle in the numbers and positions of COLs through seasonal variations in jet stream configuration. Concerning the duration of COLs, KD98 concluded that the majority of COLs lasted only 2–3 days with very few lasting more than 10 days. PV92 found that the duration ranged from 1–

17 days, although most COLs were short lived (74% of COLs lasted 3 days or less with 41% of them lasting only 1 day). They also suggested that southern COLs have a shorter life span than northern ones, a result that was confirmed by KD98. Indeed, they determined a life span for their subtropical COLs of between 2 and 4 days, whereas their polar COLs lasted longer (most of them more than 5 days). Both studies concluded that, during their early stages, COLs are either quasistationary or move erratically. PV92 found that almost half of the systems moved considerably, and KD98 concluded that about 50% of the COLs that last more than 3 days move significant distances (>600 km) between the genesis and lysis stages. The COLs tended to move northward (or northeastward) as they began to decay in strength. Some interannual variability in the frequencies of occurrence was also found in KD98. However, the short period of the KD98 hampers any generalization of results.

Studies of COL climatology were also undertaken for parts of the Southern Hemisphere. In particular, a relatively long subjective analysis was undertaken for southern Australia,<sup>57</sup> using a 14-year (1983–1996) climatology of geopotential height. The study was carried out using 3-hourly 500 hPa synoptic charts from the Australian Bureau of Meteorology archives. The authors showed that the interannual variation of COLs was particularly large. They indicated that most COLs are discernible during winter (from May to October, with an average frequency of 9.3 days per month). These Australian COLs moved either southeastward (45%) or eastward (36%) and were concentrated in a region south of lat 30°S. Some of the COLs moved very quickly, up to 10° latitude in 24 h, and some moved slowly, about 2° latitude during 1 day.

### Objective Analysis

In order to develop an objective method of detecting cut-off lows, several conditions are required.<sup>38</sup> Any objective technique should be

based on as few parameters and as little differentiation as possible and should make use of a number of grid points appropriate to the computer resources available. Furthermore, it should be intelligible in the sense that any differentiated quantities related to the initial fields should be readily apparent. It is important to develop objective approaches that yield reasonable agreement with manual analysis, although to try to reproduce subjective results precisely is pointless because manual analysis is not generally repeatable. Finally, it should be possible to apply any objective method easily to any gridded data set.

A preliminary characterization of COLs in terms of their spatial and temporal distribution was provided by Parker *et al.*<sup>53</sup> and Bell *et al.*,<sup>54</sup> who constructed a Northern Hemisphere (from around lat 20°N through 70°N) climatology of COLs using data at the 500 hPa geopotential level. Their analysis was based on data from the National Meteorological Center of the United States. The gridded data set had a resolution of 10° × 10° for Parker *et al.*<sup>53</sup> and 2° latitude × 5° longitude for Bell *et al.*<sup>54</sup> In each case, a given grid point was identified as a potential COL point if it was a geopotential minimum with respect to at least six of the eight surrounding grid points. Once this set of candidate COLs was identified, only grid points that showed a difference in the geopotential value of about 60 m in Parker *et al.*<sup>53</sup> and 30 m in Bell *et al.*<sup>54</sup> were retained. The authors made use of localized closed circulation centers for a 36-year period (1950–1985) in the case of Parker *et al.*<sup>53</sup> and for a 15-year period (1963–1977) in the case of Bell *et al.*<sup>54</sup> In both cases, detached small cyclones at 500 hPa were found primarily at middle and high latitudes. The occurrence of COLs was found to be higher within the main belt of westerlies from northeast Asia to the Gulf of Alaska near lat 50°N, and from eastern Canada/northeastern United States to southeast of Greenland and west of the United Kingdom. Their occurrence was also considerably higher throughout a band extending from the east-central Atlantic Ocean across southern

Europe to the Caspian Sea and central Asia. The authors also detected a maximum along the southern branch of the jet stream extending from the eastern Pacific into the southwestern United States. Finally, both studies found considerable monthly, seasonal, and interannual variability. COLs declined from 1950 to 1970 but increased from 1971 to 1985. A strong seasonal cycle was also found, with a maximum incidence during summer months.

In recent years, updated COL climatologies for the Northern Hemisphere have been compiled for the period from 1953 to 1999 by Smith *et al.*<sup>58</sup> and Novak.<sup>55</sup> The method used in both of these analyses relied essentially on the algorithm developed by Parker *et al.*<sup>53</sup> and Bell *et al.*<sup>54</sup> These recent studies<sup>55,58</sup> used twice-daily (0000 and 1200 UTC) 500 hPa gridded geopotential height from the NCEP–NCAR reanalysis.<sup>59</sup> One key objective of both studies was to provide greater precision for the northeastern United States, in particular for the warm season (from May to September). Favored COL areas for the cold season include the northern Pacific Ocean, the southwestern United States, north-central and eastern Canada, the North Atlantic around Greenland, and an east-west belt stretching from the Straits of Gibraltar across northern Africa and the Mediterranean into the Turkish plateau.<sup>58</sup> Moreover, these studies have found that the COL distribution is orographically and synoptically dependent. Finally, the frequency of occurrence generally increases and shifts toward the equator with the onset of winter, with the strongest signals occurring with the approach of spring.

Recent work by Nieto *et al.*<sup>26</sup> provided the first multidecadal climatological study of COLs over the Northern Hemisphere (from lat 20°N to 70°N) for the period 1958–1998. This work was based on the NCEP–NCAR reanalysis<sup>59</sup> using a 2.5° by 2.5° resolution and daily geopotential height, zonal wind, and temperature at 200 and 300 hPa. COLs were identified using an objective method that was based on the three main physical characteristics of the conceptual model of COLs.<sup>2,26</sup> The restrictive and

consecutive conditions imposed were as follows: 1) a COL was characterized by a vortex (cyclonic circulation) surrounding a geopotential minimum at the 200 hPa level and was an isolated low from the westerly circulation (using horizontal wind); 2) the equivalent thickness was characterized by a thickness ridge on the eastern flank of the center; and 3) the baroclinicity and hence the TFP had higher values eastward of the central point. This objective analysis, using a very long data set, provided a more comprehensive assessment of the issues identified by other authors in previous studies. In fact, this work confirms and reinforces previous results, namely that the three preferred areas of COL occurrence in the Northern Hemisphere are located in a) southern Europe and along the eastern Atlantic coast, b) the eastern north Pacific, and c) north China to the Siberian region extending to the northwest Pacific coast. It also confirms that the European area is the most active region in the entire Northern Hemisphere. COLs are more frequent during summer (about 50% of the total) than during winter and at higher latitudes than at lower ones. A more exhaustive analysis of the areas of occurrence revealed a two-nuclei distribution in Europe in all seasons apart from winter, a summer displacement toward the ocean in the American region, and a summer extension to the continent in the Asian region. Furthermore, about 47% of COLs formed a surface low during their cycle and 73% correspond to maxima of PV. The life span of COLs was reconfirmed as being generally less than 3 days (very few last more than 5 days), and, in general, COLs last longer when they occur at higher latitudes. Less than 20% of COLs are stationary during their life cycle, with the majority being highly mobile.

Based in part on the technique described previously, Porcú *et al.*<sup>25</sup> carried out a hybrid objective–subjective scheme to study the distribution of COLs for the decade 1992–2001 in the European area (lat 30°W–45°E and long 20°–60°N) restricted to the warm season (April to September). In this study, gridded data

were obtained from reanalysis from the European Centre for Medium-range Weather Forecast (ECMWF) (ERA-40),<sup>60</sup> with the authors constructing a 6-hourly COL database on a  $2.5^\circ \times 2.5^\circ$  resolution grid. COLs were detected with the objective algorithm described above, and the results were then post processed manually. The relevant pressure fields were analyzed subjectively in order to assign the COL center to one grid point and to ensure that two or more consecutive synoptic times of detection corresponded to the same COL. The gaps were neglected if they exceeded 12 h. The database was used to extract the geographical distribution and duration of COLs. A vertical structure analysis was also performed, characterizing the COLs from the 200 hPa level down to the earth's surface. As a consequence, the COL depth was defined as the lowest level at which a local geopotential minimum was detected during the COL life cycle. The summer months were the most active (with a peak in June). A large number of events (41%) lasted less than 1 day and the number of detected COLs decreased monotonically with increasing life span. Geographically, the following pattern was determined: a local maximum was located over the western Iberian peninsula in the Atlantic, a second maximum toward the north of Spain/southern France, and a third one from the Ionian Sea to Anatolia and the Black Sea. Furthermore, by distinguishing between COLs with a life span more than 1 day (HCOL) and less than 1 day (LCOL), it was determined that while HCOLs are preferably located over the western Portugal coast, the distribution of LCOLs showed two lesser peaks, one over the Iberian peninsula and one over the western Black Sea. The results showed that about 60% of the detected COLs had an associated closed geopotential contour at surface level.

Objective methods have also been used to study spatial and seasonal distributions of COLs over the Southern Hemisphere. In particular, Fuenzalida *et al.*<sup>61</sup> studied the occurrence of COLs at 500 hPa using

four-times-daily NCEP–NCAR reanalysis fields for the 31-year period from 1969 to 1999. They used a mixed method based on an objective detection of lows combined with a visual inspection. The region under analysis covered the entire Southern Hemisphere between lat  $10^{\circ}$  and  $60^{\circ}$ S. COLs tended to occur in a belt between lat  $20^{\circ}$  to  $50^{\circ}$ S with a maximum density at lat  $38^{\circ}$ S and with a higher frequency around the three main continental areas and a lower frequency over the oceanic regions. Using three equally spaced sectors covering the whole Southern Hemisphere, the authors showed that only 10% of the COLs were found in the African sector, with 48% in the Australian sector and 42% in the South American sector. The COLs showed a strong seasonal cycle in South America and Africa (with a lower occurrence during summer), while in the Australian area they occurred fairly steadily throughout the year. The authors further noted that over South America, the dissipation of COLs was a more common feature than their generation, with the opposite behavior occurring over the Australian continent. Close to South America, a statistically significant increase in the number of COLs over time was observed at the 500 hPa level, with a higher frequency of COLs being generally observed after 1990. Typical life spans of COLs were found to be similar to those found for COLs in the Northern Hemisphere, with most COLs lasting for a short time; only 10% lasted longer than 5 days. The frequency distribution of intensity (maximum value of geopotential on each COL track) showed no geographical variation.

Using smaller areas, such as the subtropical coast of Chile<sup>62</sup> or southern South America,<sup>63</sup> two climatologies were developed using NCEP–NCAR reanalysis during the periods 1979–1996 and 1979–1988, respectively. The first one identified COLs using the meridional geopotential gradient at 500 hPa, calculated as the difference between geopotential heights over lat  $30^{\circ}$ – $35^{\circ}$ S, long  $80^{\circ}$ – $75^{\circ}$ W and lat  $35^{\circ}$ – $40^{\circ}$ S, long  $80^{\circ}$ – $75^{\circ}$ W. Negative values were

considered as a COL. The typical intense seasonal variability was found (ranging from two to 15 events), with the austral spring being the most frequent season. The second climatology was developed using an algorithm based on a COL conceptual model.<sup>26</sup> The selected domain extended from long  $100^{\circ}$ W to  $20^{\circ}$ W and from lat  $15^{\circ}$ S to  $50^{\circ}$ S. The highest frequency of occurrence was over the Pacific area (44%), followed by the Atlantic (30%) and continental areas (26%). COLs were more frequent in the austral autumn (in particular over the coast of Chile) and less frequent during summer. A shorter duration of COLs (2–3 days) was also detected, but over continental areas COLs were of longer duration.

The COL climatologies presented so far are essentially based on geopotential height. A different approach is also possible because COLs are characterized by an anomalous lower tropopause, which induces higher values of PV within the COL core. This feature was used to identify COLs over the northern Atlantic during the decade from 1989 to 1999 by Hernández<sup>56</sup> and Cuevas and Rodríguez.<sup>14</sup> Both studies used the operational ECMWF 12-hourly data at 315 K, 320 K, 325 K, and 330 K, with a horizontal resolution of  $1.25^{\circ} \times 1.25^{\circ}$ . The criterion used to locate COLs was the same for both studies, namely that a COL was defined as a closed contour on isentropic surfaces of 2 PVU, with an inner maximum of at least 4 PVU, and covering a minimum extension of  $30^{\circ} \times 30^{\circ}$ . The results obtained using this approach confirm that the highest frequency of COLs can be observed in the vicinities of the Iberian peninsula during all seasons, with two peaks of occurrence, one over southwestern Iberia and the other over southern Iberia (this maximum did not appear in Ref. 14). The monthly occurrence was higher during the warm season, with June and July being the most active months, which was in agreement with the highest values of tropospheric ozone measurements indicating STE. Over southeastern Europe, two kinds of behavior were described concerning the movement of COLs, namely (1)

that they were either quasistationary or (2) that they moved in a cyclonic sense with a mean gyre of  $20^\circ$  in 12 h and a maximum movement of  $8.75^\circ$  in longitude and  $6.25^\circ$  in latitude in 12 h. As in previous climatologies, the interannual occurrence showed large variability, with an absolute maximum (minimum) taking place around 1993 (1998).

Finally, Wernli and Sprenger<sup>6</sup> presented a climatology of potential vorticity (PV) streamers and cut offs for the Northern Hemisphere defined on isentropes from 295 K to 360 K. Their analysis covered the period from 1979 to 1993 and was based on the shorter ERA-15 reanalysis data set from the ECMWF. In their case, COLs were identified as closed isolines of the two-PVU contour on the previously mentioned isentropes. One of their main findings relating to the spatial distribution of COL events revealed a pronounced zonal asymmetry and a clear change of frequency maxima with altitude. For instance, at 300 K and during winter, most COLs were found over the western side of Canada and Siberia (near lat  $50^\circ$ – $60^\circ$ N), whereas on higher isentropes the frequency maxima were shifted further to the south and were generally found at the downstream end of the North Atlantic and Pacific storm tracks. With respect to continental areas, the Mediterranean stands out as a region with a particularly high number of COL episodes. In addition to the pronounced geographical variability on specific isentropic surfaces, a distinct seasonal cycle can be discerned. This cycle is attributed mainly to the seasonal shift of the isentropic surfaces themselves. In fact, if the COL frequency is considered as a function of latitude, irrespective of the vertical altitude, a fairly robust pattern with almost no seasonal cycle emerges.

### Common Results of Previous Climatologies

Taking into consideration all the studies summarized above for the Northern Hemisphere at extratropical latitudes, it can be seen that COLs

are more frequent in summer than in winter and that they occur preferably near the major troughs of the large-scale circumpolar flow. Almost all the studies found commonly favored regions of occurrence, namely southern Europe and the eastern Atlantic coast, the eastern North Pacific, and the north China–Siberian region extending to the northwest Pacific coast, with Europe being the region of most common occurrence. Their duration is typically from 2–3 days with few lasting more than 5 days. Analyses of larger data sets of several years or more also found very large interannual variability in the occurrence of COLs at the annual and seasonal scales, although without any significant trends. Several major large-scale modes of variability in atmospheric circulation seem to have an impact on the occurrence of COLs. In particular, blocking events, the North Atlantic Oscillation (NAO), the El Niño–Southern Oscillation (ENSO), and the persistence of the stratospheric polar vortex may influence the occurrence of COLs.<sup>3,64</sup> Despite the few (and only empirical) studies that look for the influence of these modes on COL occurrence, there are physical reasons that provide support for this relationship. Blocking events and COLs are both associated with the occurrence of important disruptions of the upper tropospheric jets as well as being associated with strong meridional components and even with the bifurcation of the jet and the appearance of double jets.<sup>65,66</sup> Blocking events and COLs, therefore, tend to occur mainly during winter. The relationship of the NAO or ENSO with the intensity and zonality of the jet flow is well known.<sup>67,68</sup> The negative (positive) ENSO and NAO phases are related to the appearance of weaker (stronger) jets and to a higher (lower) probability of COLs occurring. Furthermore, there are dynamic reasons for thinking that the occurrence of COLs could be influenced by the persistence of the stratospheric vortex (the quasisteady summer-like state after the decay of the vortex with strong weakening of the westerlies favors COL development, and the fact that remnants of the vortex survive as coherent PV structures for

around 2 months for early breakup years<sup>69,70</sup>). As a consequence, COL events appear to be more frequent during the late spring and in summer months for those years characterized by an earlier vortex decay.

## **Climatologies Based upon the Conceptual Model and Potential Vorticity**

### **Data**

Three climatologies of COLs were calculated using two reanalysis data sets, namely the ERA-40 and NCEP–NCAR. ERA-40 reanalyses<sup>60</sup> were produced by the ECMWF in the late 1990s, using a T106 model resolution with 60 vertical levels and the optimum interpolation data assimilation technique. The NCEP–NCAR reanalysis<sup>59</sup> is an intermittent data assimilation scheme performed with a T62 model with 28 vertical sigma levels and the operational statistical interpolation (SSI) procedure for assimilation. The first two climatologies were built from 6-hourly data from the ERA-40 and from the NCEP–NCAR and based on the conceptual model of COL developed by Nieto *et al.*<sup>26</sup> This approach uses geopotential, zonal wind, and daily temperature data from 200 and 300 hPa with a 2.5° by 2.5° resolution. Those cut-off systems found north of lat 70°N or south of lat 20°N were not included in the study. The reason for excluding systems north of 70° was in order to eliminate the main polar vortex, and the reason for excluding cut-off systems south of 20°N was the small probability of their occurring, despite the fact that this could be physically meaningful as has been shown in previous climatologies. The time periods covered by the analyses varied, depending on the availability of data. While the ERA-40 data were only available from January 1958 to December 2002, the NCEP–NCAR data set extended from January 1948 to December 2006. The third climatology was developed using potential vorticity (PV) as the physical parameter of diagnosis, us-

ing as a basis the methodology developed by Wernli and Sprenger.<sup>6</sup> This analysis is applied only to the ERA-40 data set from the ECMWF covering the period from January 1958 to December 2002. The required fields (horizontal wind components, temperature, and geopotential) are available every 6 h on 60 vertical levels from the surface up to 10 hPa and were interpolated onto a regular grid with a 1° horizontal resolution. Secondary fields, such as potential temperature and PV, were computed on the original hybrid model levels. Finally, the PV field was interpolated to a stack of isentropic levels from 300 to 350 K at 10 K intervals (see Fig. 11 for an illustrative example showing the heights at which these isentropic surfaces are located).

### **Climatology Based on the Conceptual Model**

COLs are identified by means of three consecutive and restrictive steps that are based on the physical characteristics of the conceptual model of COLs described in section 2 and by Nieto *et al.*<sup>26</sup> (hereafter, NAL). The condition of a minimum of geopotential height field of 200 hPa and the isolation from the general circulation pattern of westerlies in the upper troposphere was the first imposed restriction used in considering a grid point as a part of a possible cut-off low. At each 6-h interval, a given grid point was therefore identified as a geopotential minimum if it is a minimum (within a 10 gpm threshold) with respect to at least six of the eight surrounding grid points. Once this set of COL points was chosen, we retained only the grid points that showed changes in the direction of the 200 hPa zonal wind at either of the two grid points situated immediately to the north of that grid point. The next required condition for a COL was that it should have a greater equivalent thickness (computed between two pressure levels, in this case 200 and 300 hPa) to the east of its central point than this value at its center. Finally, the grid point immediately to the east of a candidate COL point

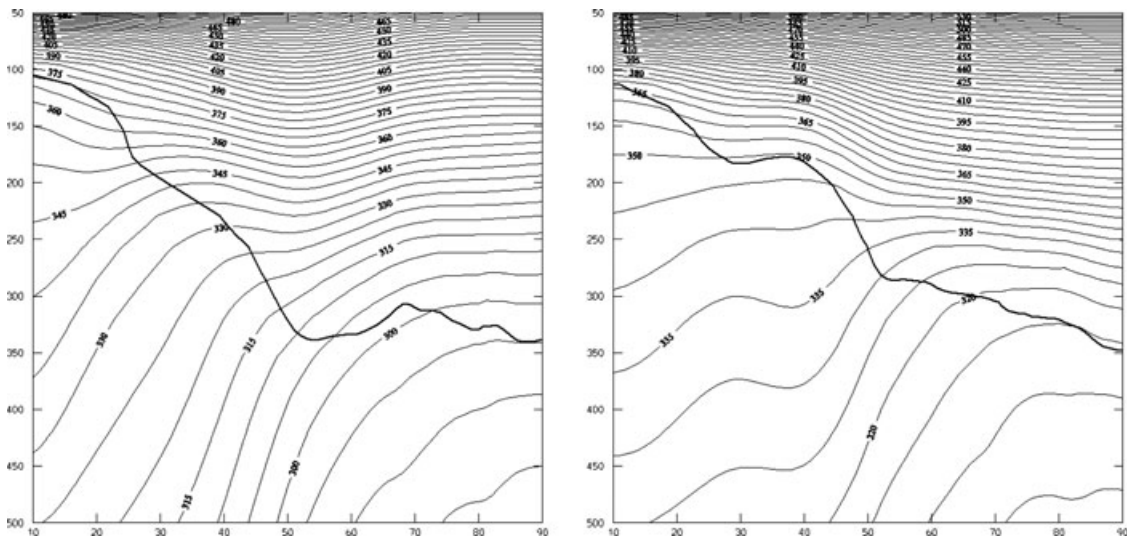


**Figure 11.** Potential temperature (corresponding to isentropic surfaces) and tropopause (two-PVU isosurface) along the 50°W meridian for January (left) and July (right). Of particular interest to this study are the isentropes between 300 and 350 K. The horizontal axis is the geographical latitude, the vertical axis the pressure (in hPa).

was required to have a TFP higher than that at the COL point in order to locate the frontal baroclinic zone. The temperature at 200 hPa was used to calculate the TFP in our analysis. If all these conditions were fulfilled, the analyzed grid point was considered to be a COL point. It should be noted that this algorithm is essentially identical to the one previously developed by NAL but makes use of 6-hourly data instead of one single daily value. Some other refinements were made to the NAL method in terms of the method of calculating the TFP, thus achieving better resolution in temperature gradients. Some of the COL points detected were probably the same COL observed over consecutive days. In NAL, several conditions were imposed to determine where the same COL had been identified more than once, but in these climatologies the plots and statistics will be presented for all points that fitted the COL conditions outlined above. It should be noted that, unlike in NAL, systems that lasted only 1 day or less were not excluded from the analyses. With these additional steps, we are confident that both the COL databases derived from ERA-40 and NCEP–NCAR are now more pre-

cise and more extensive than those obtained in NAL, mostly because of the higher temporal resolution and the extended time period considered.

### Case Study

The possibility of wrongly identifying a COL was minimized by imposing the consecutive and restrictive conditions described above, but the possibility nevertheless still existed of failing to identify systems that, in a subjective analysis, would have been considered as cut-off lows.

Figure 12 summarizes the procedure imposed at each step for a real example of a cut-off low. The method identified a cut-off low on May 13, 1992 that lasted only 6 h. Subjective analysis might identify this COL as ending on May 15, 1992, but by applying our methodology, days after May 13, 1992 were not considered as cut-off low days because they did not fit all our imposed conditions, which must be satisfied simultaneously. In particular, the most restrictive conditions, concerning the minimum thickness and the TFP, were not satisfied. On May 13, 1992, 1200 UTC, a minimum of geopotential over the southern Italian

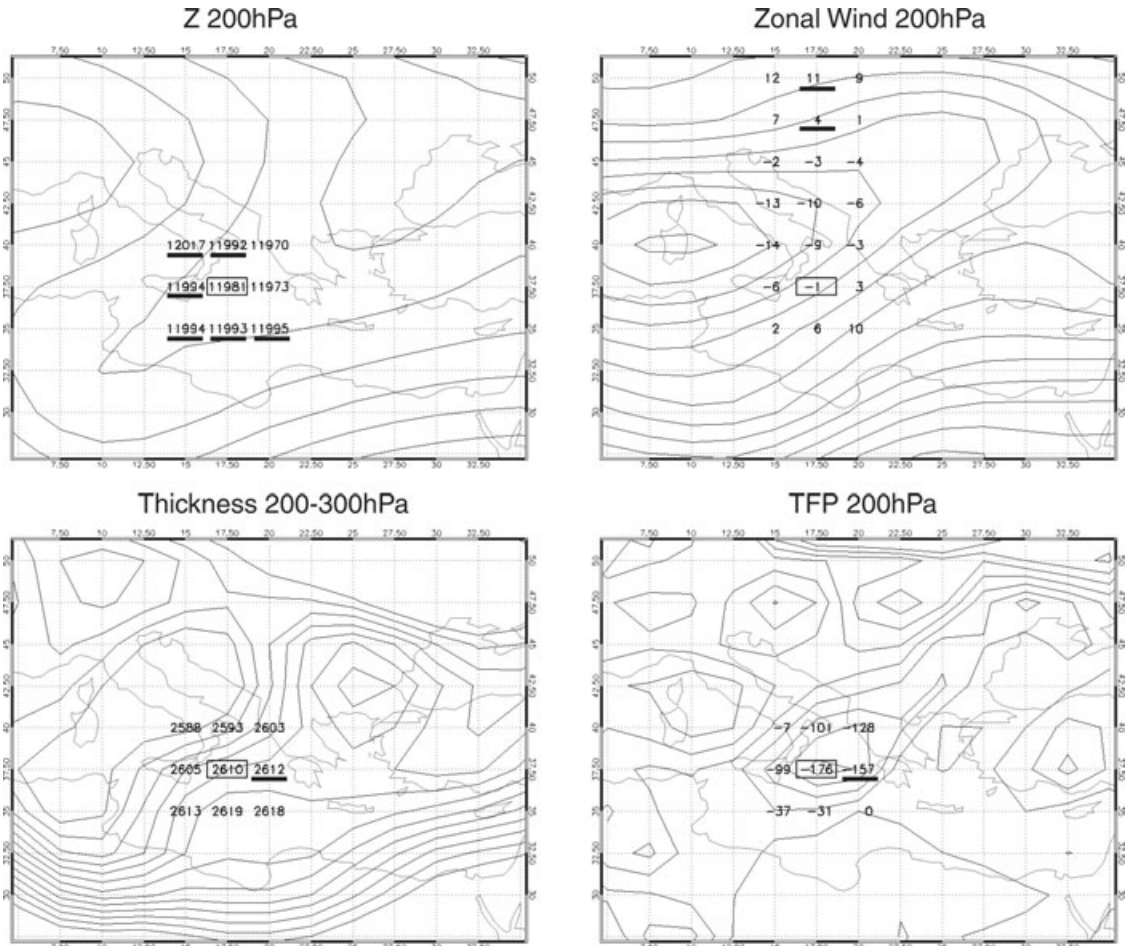


**Figure 12.** Cut-off low detected on 13 May 1992 at 12 UTC that met all the criteria imposed by the objective method. The box shows the COL point detected and the underlining grid point fits the imposed condition.

peninsula was detected at 200 hPa (left top panel of Fig. 12). The evolution of the COL at that moment corresponded with the upper-level trough stage and the initial tear-off stage, but the circulation was already detached from the westerlies, as shown by the zonal wind patterns at 200 hPa (right top panel). The baroclinic boundary was detected to the east of the selected COL point (bottom panels). Only 6 h later, only two out of four conditions were fulfilled, which explained why this COL had a life span shorter than 1 day using our new climatology. Later, it will be shown that this COL nevertheless complied with the conditions imposed in the diagnosis of the PV.

### Climatology

This section presents the two climatologies that were based on the conceptual model of COLs over the Northern Hemisphere (lat 20°–70°N). Figure 13 shows the seasonal frequency with which a cut off is found over a grid point using the ERA-40 data set (hereafter, ERANAL), and Figure 14 shows the equivalent results using the NCEP–NCAR data set (hereafter NCEPNAL). The gray scale refers to the percentage per 1000 (‰) of COL points over a grid point, counting all the hourly occurrences. This display differs significantly from those used in previous studies of spatial distribution, which

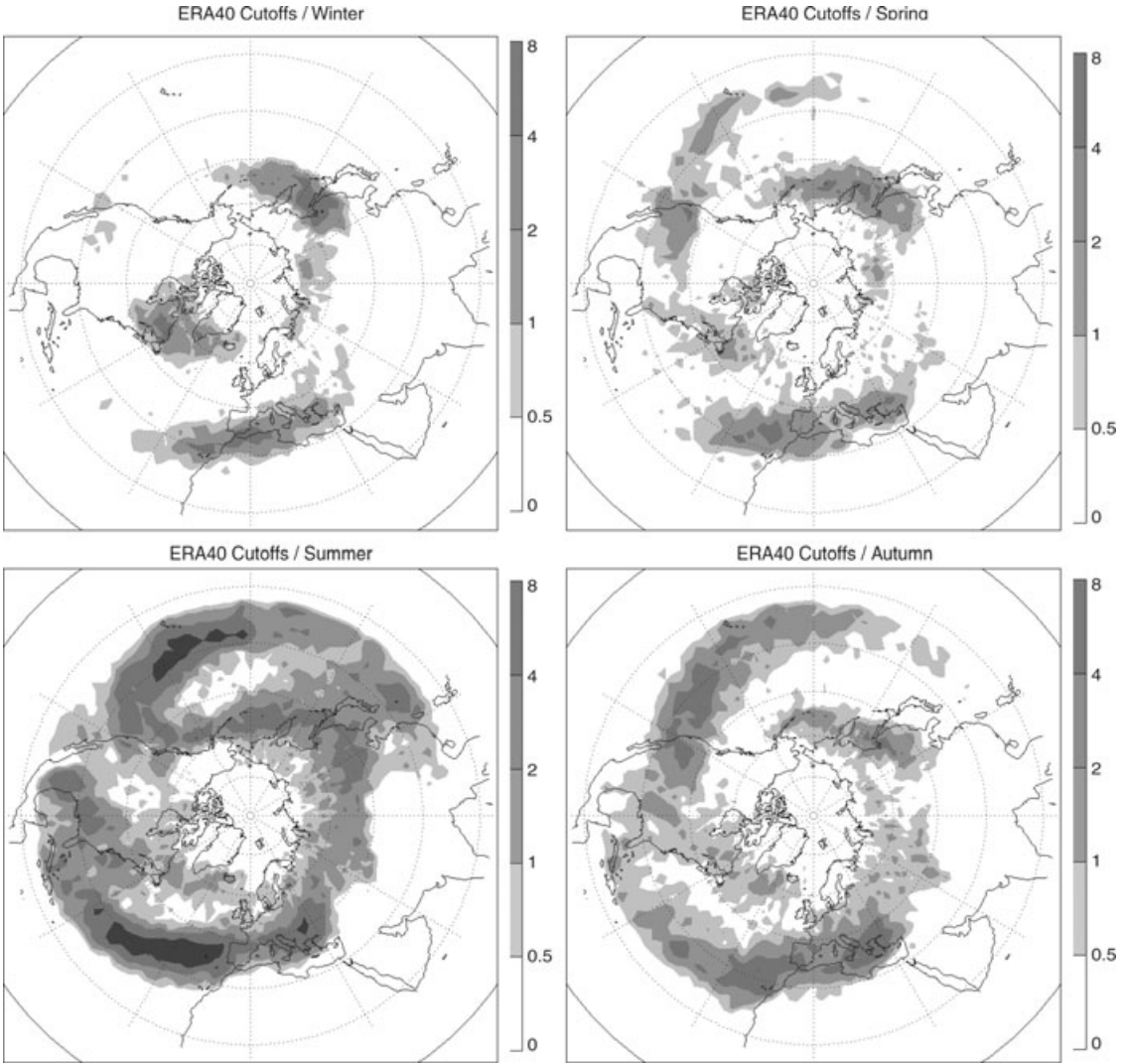


**Figure 13.** ERA-40 (1958–2002) climatology cut-off lows (ERANAL) in a  $2.5^\circ \times 2.5^\circ$  grid for winter, spring, summer and autumn. The gray shading gives the percentage per thousand (%) of time for which a grid point is part of a cut off.

showed only the frequencies of the first day of COL occurrence.

The most important finding is that the geographical distribution of COLs is very similar in both climatologies and is also coherent with what was obtained in NAL, with most of the cut-off lows being concentrated in three main areas. These areas are (1) southern Europe and the eastern Atlantic coast, including the Mediterranean and northern Africa, (2) the eastern North Pacific coast and north-

east United States, and (3) the north China–Siberian region extending to the northwest Pacific coast.

Another significant outcome is that for both climatologies, the position of the COLs changes coherently from season to season. COLs are much more common in summer [June to August (JJA)] (lower left panel) than in winter [December to February (DJF)] (upper left). We calculate that 43% (41%) of these COLs take place during summer and 15% (17%) during winter,

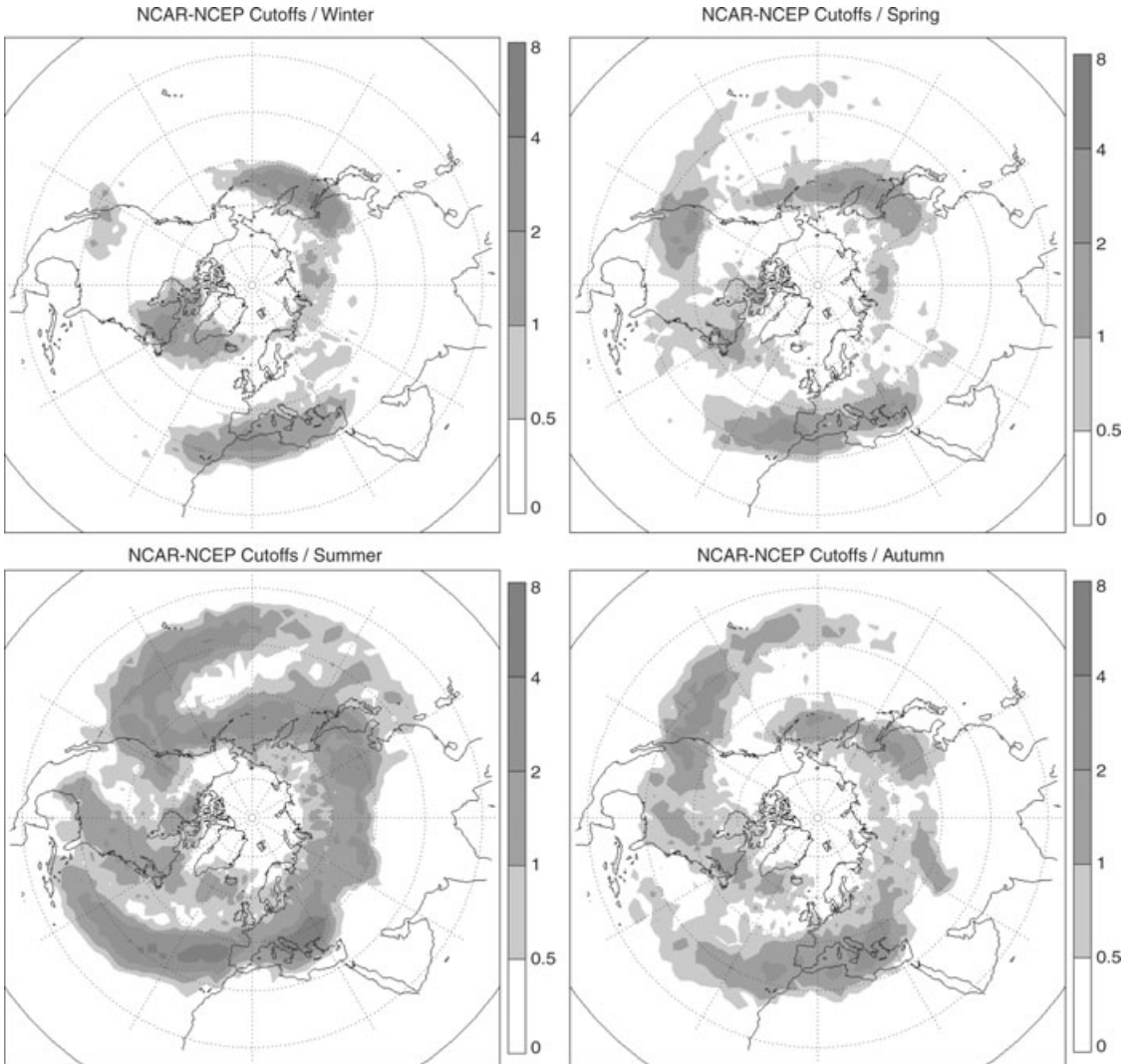


**Figure 14.** NCAR-NCEP (1948–2006) climatology cut-off lows (NCEPNAL) in a  $2.5^\circ \times 2.5^\circ$  grid for winter, spring, summer, and autumn. The gray shading gives the percentage per thousand ( $\text{‰}$ ) of time for which a grid point is part of a cut off.

using ERANAL (NCEPNAL). During summer, most COLs are found in a bipolar band with two centers for both climatologies, one spanning the middle North Atlantic to the Iberian peninsula and another centered over the eastern Mediterranean, reaching values with peaks around 6.5 $\text{‰}$ . The maximum of occurrence over the Atlantic area has a larger zonal extension for ERANAL than for NCEPNAL, with the former starting from the mid ocean and the latter starting near the Iberian peninsula. The

bands detected over the western Pacific coast of China and over the eastern Pacific coast of North America have similar extensions in both climatologies, with a region of higher COL occurrence for ERANAL over the mid Pacific ( $>4\text{‰}$ ). During winter the pattern is more similar between climatologies than during summer. For ERANAL the western Pacific coast of China is the area of higher occurrence, and COLs are more frequent over the northern Atlantic coast of North America than the eastern

Pacific coast of North America. Comparing the three main regions, the eastern Pacific coast of North America is where COL occurrence is most unstable—limited to the Pacific coast during winter and then expanded and displaced westward during the remaining seasons. This is most probably because of the strong seasonal cycle that is imposed by the meridional displacement of the jet stream (the main production mechanism that is responsible for cut-off low formation) over the areas most prone to COL formation. Over the European region, the bipolar structure that is found in summer disappears during winter and COLs tend to occur toward lower latitudes than during summer. The spring and autumn seasons are characterized by a transitional structure pattern.

### Climatology Based on Potential Vorticity

Stratospheric and tropospheric cut offs were identified using the following algorithm: (a) first, the PV on an isentropic surface is separated into parts with PV larger and smaller than 2 PVU; (b) based upon this distinction, a unique label is attributed to each connected patch of high ( $>2$  PVU) and low ( $<2$  PVU) PV air, resulting in a clustering of stratospheric and tropospheric air masses on that isentropic surface; (c) the largest patches of connected high and low PV air are discarded because they correspond to the stratospheric and tropospheric PV reservoirs, respectively; (d) the remaining patches are saved as stratospheric (for high PV) and tropospheric (for low PV) cut offs. Note that this algorithm is somewhat different from the one recently applied in Wernli and Sprenger<sup>6</sup> (hereafter WS). A minor difference applied in this study is in relation to an area threshold. If a connected tropospheric or stratospheric patch is smaller than  $5 \times 10^4$  km<sup>2</sup> or larger than  $1000 \times 10^4$  km<sup>2</sup>, it is discarded in this data set. The former criterion guarantees that minor and most probably spurious cut offs with a weak dynamic impact are neglected, whereas the latter criterion is a “security check” to ensure that a large part of the stratospheric (or

tropospheric) reservoir has not split from the main body, which of course has nothing to do with the traditional view of cut offs.

As was the case in WS, a clear distinction between stratospheric cut offs and ephemeral diabatically produced PV anomalies is difficult to obtain and would require the computation of trajectories to check for PV conservation. However, such an analysis is computationally expensive and has been performed in the study reported herein. As will be shown later, it appears that at the lower isentropes considered, some of the PV cut offs identified do appear to be related to the surface topography. However, because of their stationary nature, they do not get mixed up with the real stratospheric cut offs. A simple, but rather rough, elimination of surface-induced cut offs is implemented in the new algorithm. All cut offs must be characterized by a minimum distance of 75 hPa from the COL grid point with the highest pressure value to the surface pressure, otherwise they are neglected in the climatology.

### Case Study

In this section, the same case study of cut-off formation that was assessed previously (Fig. 12) is discussed, but this time within the framework of the PV-detecting approach. Figure 15 shows an isentropic PV (IPV) map on the 320 K isentropes. On May 13, 1992, 0600 UTC, a narrow filament of high-PV air extended from Poland southwestward to Greece and southern Italy (left panel). While the northern stratospheric high-PV reservoir remains a compact body, the filament shows a tendency to cut off. This feature is clearly discernible in the narrowing of the filament to the west of the Black Sea. Indeed, 36 h later (right panel), the southernmost parts of the filament were completely decoupled from the stratospheric reservoir and showed as a distinct PV cut off. Since this was high-PV air of stratospheric origin, it is known as a stratospheric cut off. The wind vectors are also included in Figure 15. In accordance with the invertibility and partitioning principles of the PV perspective, as summarized by Hoskins

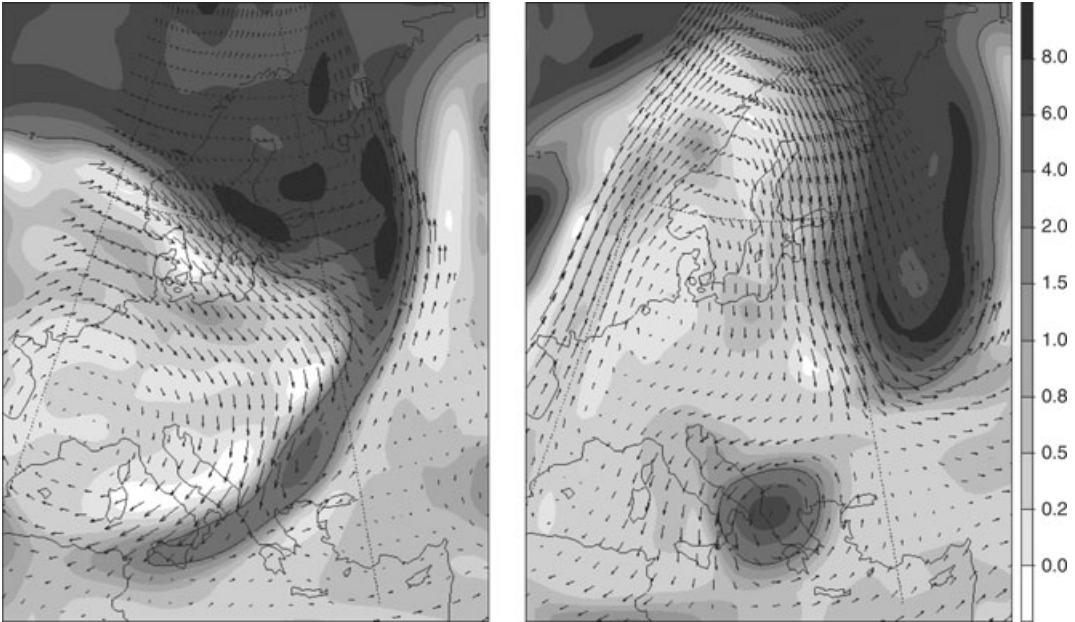


**Figure 15.** Isentropic potential vorticity (IPV) map on the 320 K isentrope for 13 May 1992 at 06 UTC (left) and 14 May 1992 at 18 UTC (right). Potential vorticity values are given in PVU ( $1 \text{ PVU} = 1 \times 10^{-6} \text{ m}^2 \text{ s}^{-1} \text{ K kg}^{-1}$ ). Additionally, the wind vectors for the 320 K isentrope are overlaid on the figure, with the wind speed (in m/s) shown on the lower right corner. The dynamical tropopause (two-PVU isosurface) is marked by the bold black line. Note the slightly different geographical region shown in the two panels.

*et al.*,<sup>5</sup> the stratospheric PV cut off is associated with a cyclonic wind field.

Although a clear indication of the stratospheric origin of the Mediterranean PV cut off is obtained from this Eulerian approach, especially if intermediate time steps are also considered, a Lagrangian approach reveals its northern source region even more clearly. To this end, air parcels within the stratospheric cut off (Fig. 15, right panel) were set as starting points for a backward trajectory calculation. Figure 16 shows the trajectories as calculated by ECMWF winds and by the 3D Lagrangian trajectory tool LAGRANTO<sup>71</sup> that involves the calculation of extensive coherent ensembles of trajectories with a 6-h time step. Trajectories emanating from the affected area are evaluated over the subsequent 72 h—a time period which includes a phase of upper-level PV isolation.

The air parcels moved in an almost zonal flow pattern over Scotland and Denmark, before turning southward. They quickly reached

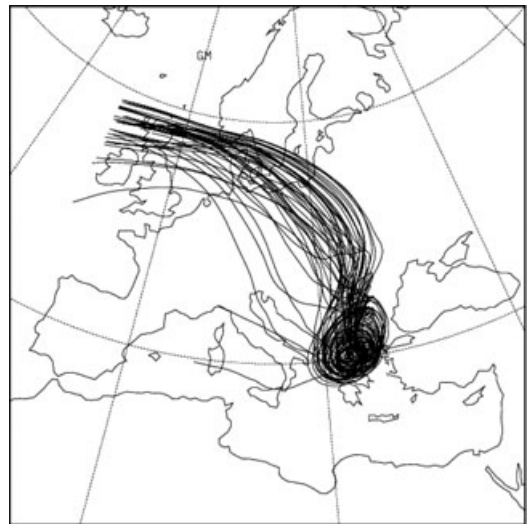


**Figure 16.** Backward trajectories using LAGRANTO from the stratospheric cut off in Figure 15. The trajectories start at 14 May 1992, 18 UTC and extend 72 h backward in time.

a location over Greece and were then “captured” in the cyclonic flow around the PV cut off.

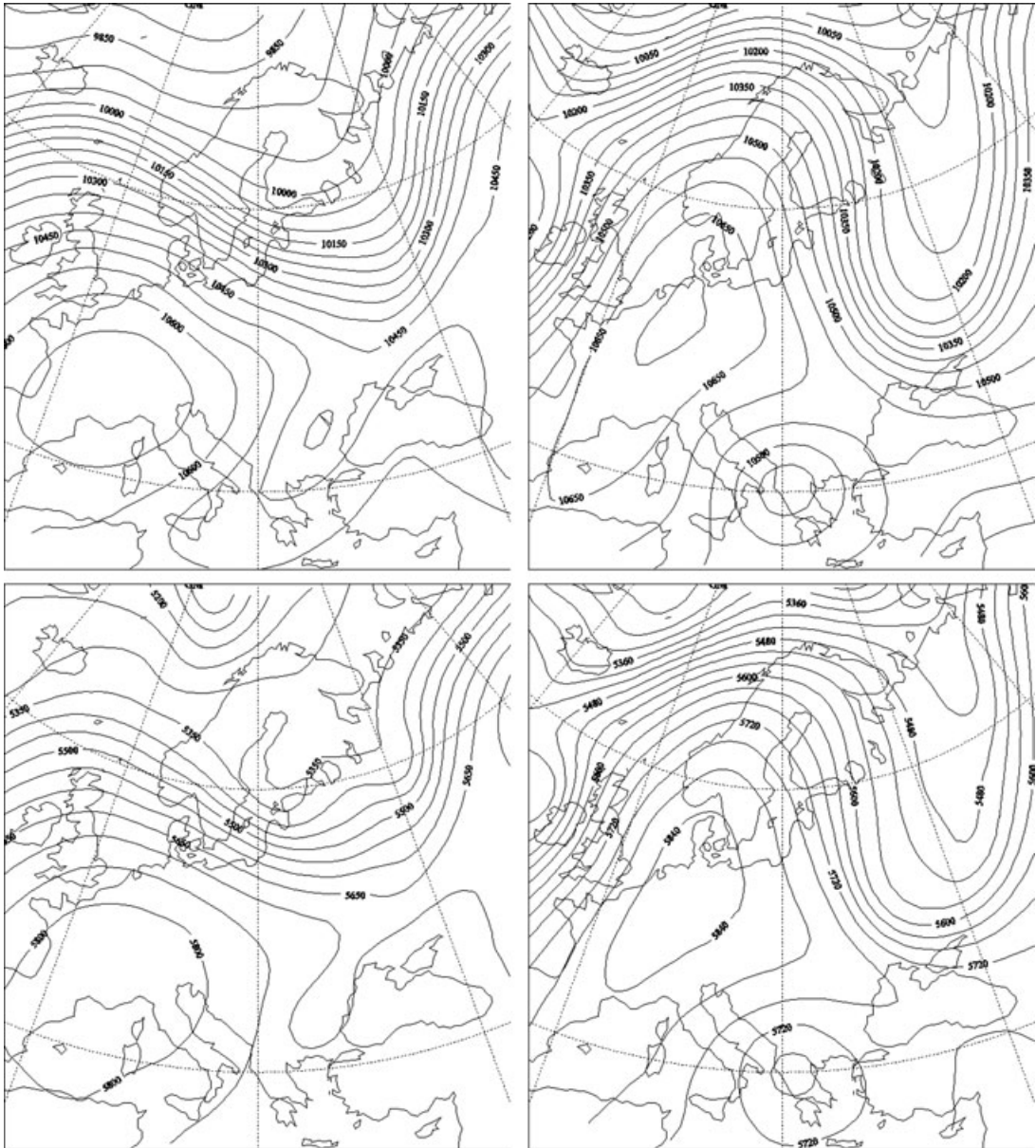


**Figure 17.** Geopotential height at 13 May 1992, 06 UTC (left) and 14 May 1992, 18 UTC (right), and for the two levels 250 hPa (upper) and 500 hPa (lower).

Finally, it is worthwhile considering the traditional view of this PV cut-off event, i.e., its manifestation as a closed contour of geopotential height. This is shown in Figure 17 where the geopotential height at 250 and 500 hPa is plotted for the two times shown in Figure 15 (May 13, 1992, 0600 UTC and May 14, 1992, 1800 UTC). For the first of these, a closed isoline of

geopotential height at 250 hPa may be observed to the west of the Black Sea, showing the tear-off stage. This small-scale cut off coincides with the southern parts of the narrow PV filament in Figure 15. At the lower level (500 hPa), no closed contours can be seen, which is indicative of the shallow vertical extent of the 250 hPa cut off in this stage prior to the cut-off phase. In

sharp contrast to this, for the following day, closed isolines of geopotential height are found at all levels, from 250 hPa down to 500 hPa. Hence, during the cut-off stage, this COL is characterized by a significant vertical depth.

The above example clearly illustrates the following important features: (a) an upper-level PV cut off might be associated with a geopotential cut-off low; (b) the opposite is not necessarily the case, as for example the narrow PV filament (the stratospheric PV streamer) is also associated with a closed geopotential cut off, albeit at a smaller scale; and (c) a substantial upper-level PV cut off is associated with a geopotential cut off extending over a significant part of the troposphere (at least from 250 down to 500 hPa in this case). Considering the mismatch between the two methods, an obvious question arises in relation to the physical relevance of either definition. The physical meaning of geopotential cut offs was discussed in an earlier section. Here, some additional attention is given to the meaning of PV cut offs. One key aspect of PV theory is the invertibility principle. This states that the PV distribution in the interior of a domain is sufficient to derive the wind and temperature field in the domain, provided that some boundary conditions are specified and a suitable relationship between the geopotential height field and the wind field is assumed (this relationship is often referred to as the balance condition underlying the PV inversion). In this PV framework, it is relatively straightforward to show that a positive upper-level PV anomaly (for instance, a stratospheric PV cut off) is associated with a cyclonic wind field and a decreased temperature below the anomaly. It is particularly important that the impact of the upper-level PV structure should not be restricted to these upper levels but induces wind and temperature anomalies below and above them as a consequence of the elliptical character of the PV inversion problem. Through this mechanism, a sufficiently strong upper-level PV cut off must coincide with some vertically coherent anomaly of horizontal wind and temperature. In summary, it is clear that

a sufficiently strong upper-level PV cut off coincides with a geopotential cut off that extends over a significant part of the troposphere.

### *Climatology*

We now present a climatology of stratospheric PV cut offs from 1958 to 2002. Figure 18 shows the seasonal distribution of frequencies of stratospheric PV cut offs. The most striking aspect is the clear deviation from zonal symmetry. During winter (upper left panel), most stratospheric PV cut offs are found in an almost zonal band that extends from the Azores to the eastern Mediterranean. Values of peak frequency in this band reach up to 4%. Further downstream, this band extends as far as the Pacific coast of China, although with a considerably reduced amplitude. A secondary maximum is discernible over the west coast of North America, extending westward to the eastern Pacific and eastward almost to the east coast. One possible explanation for this geographical distribution is linked to the North Pacific and Atlantic storm tracks. It is well known that the exit regions of these two storm tracks<sup>6</sup> are affected greatly by nonlinear distortions of the two-PVU isoline on an isentropic surface, i.e., by the breaking of Rossby waves. As shown in Figure 15, the associated PV streamers quite often break up, forming stratospheric PV cut offs. It is worthwhile mentioning that the PV cut-off maxima are found slightly to the south of the main region that contains breaking Rossby waves. During spring (upper right panel), the geographical patterns remain essentially the same as in winter, with an intriguing third maximum appearing over Japan. Summer (lower left panel) is associated with the highest PV cut-off frequencies, with peak values of 8% very often being surpassed. Note also that the geographical pattern is much more zonally symmetric, being shifted significantly to the north compared to during winter. Given that the climatology is calculated on an isentropic surface (320 K in this case), the seasonal shift of the PV cut off simply reflects the seasonal shift of the isentropic surface (see also

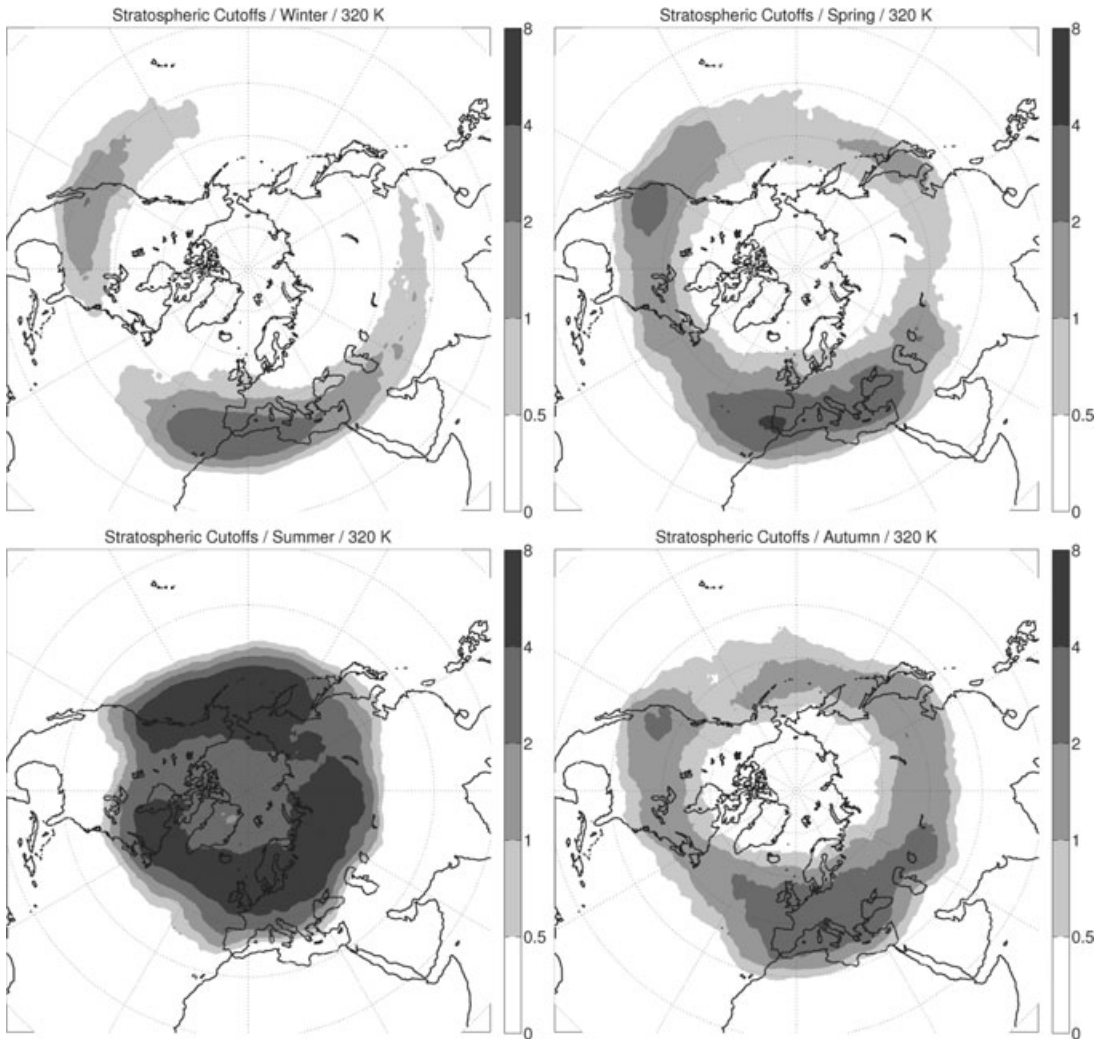


**Figure 18.** ERA-40 (1958–2002) climatology of stratospheric PV cut offs on the 320 K isentropes for winter, spring, summer, and autumn. The gray shading gives the percentage (%) of time for which a grid point is part of a PV cut off.

Fig. 11). Indeed, as a result of this seasonal shift, it is essential that other isentropic surfaces are considered, in order to obtain a comprehensive view of the distribution of cut-off formation. Finally, autumn (lower right panel) is again very similar to spring.

The stratospheric PV cut-off climatology on the 340 K surface is presented in Figure 19 in which it can be seen that the maxima are located further to the south (consider the intersection of the 2-PVU isoline with the 320 and 340 K isolines in Fig. 11). In addition to

this southward shift, a westward shift of maxima can be seen relative to their equivalent positions for the 320 K surface. For instance, the spring maximum over the west coast of the United States (at 320 K) can now be found in the mid Pacific (at 340 K) and the autumn maximum over Europe and the Mediterranean (at 320 K) is now shifted to the mid Atlantic. It should also be noted that the summer distribution pattern on the 340 K surface is significantly different from the much more zonal pattern found on the 320 K surface.

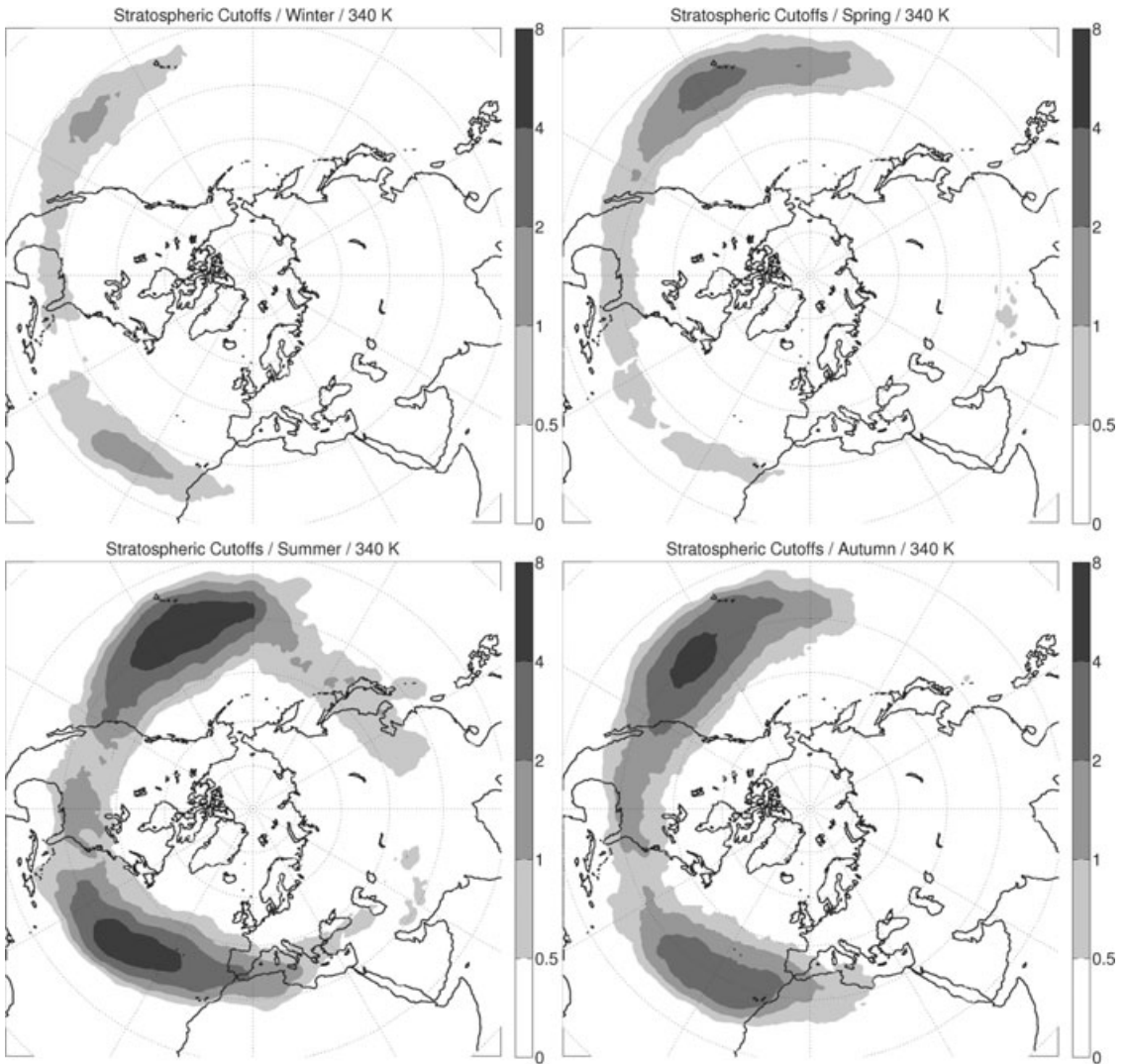


**Figure 19.** ERA-40 (1958–2002) climatology of stratospheric PV cut offs of the 340 K isentropes for winter, spring, summer, and autumn. The gray shading gives the percentage (%) of time for which a grid point is part of a PV cut off.

### Comparison and Conclusions

Preliminary inspection of the two climatologies described in Section 4 shows good agreement in terms of their spatial distribution. A more rigorous comparison between these approaches can be obtained by plotting in a single figure the seasonal percentage of COLs detected in the areas of maximum COL occurrence (Fig. 20). This analysis is limited to the common period of input data, i.e., January 1958–December 2002 and the common

latitude band between 20°N and 70°N. The ERANAL (gray areas) and NCEPNAL (continuous black line) climatologies agree quite remarkably, with the few differences restricted to their extent; the main areas of occurrence, namely the European area, the Asian area, the North American Pacific, and Atlantic areas were detected equally using both data sets. The detection of these areas of main COL occurrence in the stratospheric WS climatology depends on the isentropic level under consideration. Several isentropic levels (310, 320, 330,

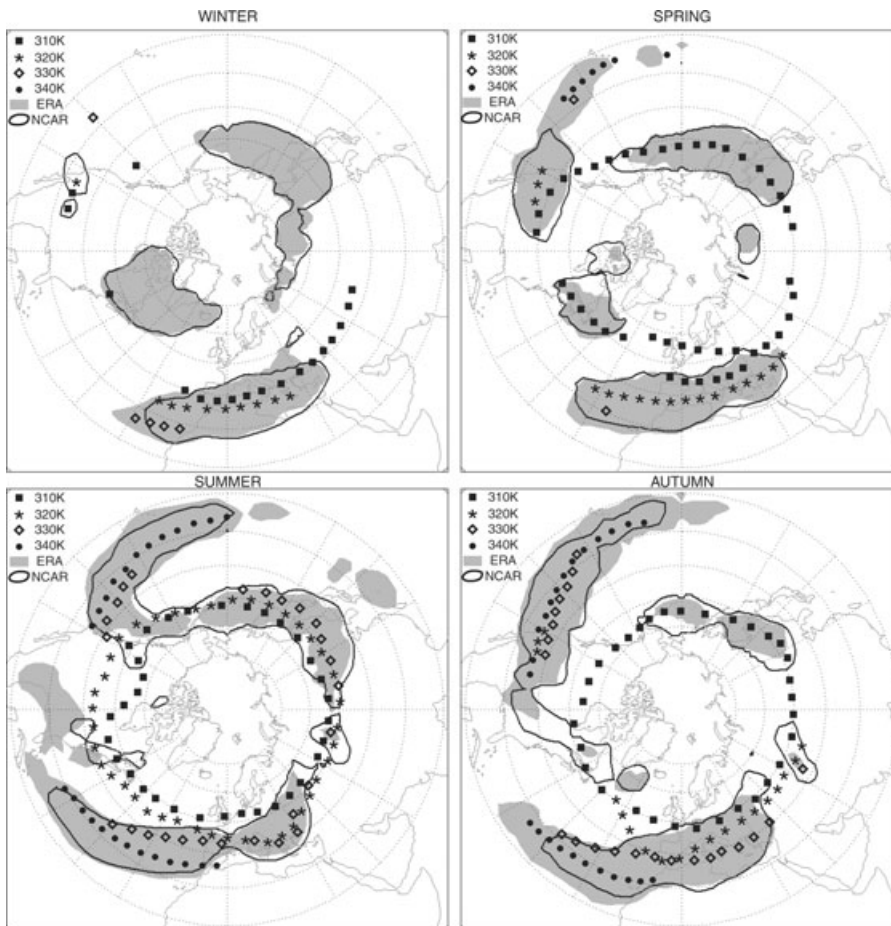


**Figure 20.** Comparison between seasonal COL climatologies. Gray areas are ERANAL climatologies, the black line denotes NCAR-NCEP NAL climatologies, and squares, asterisks, rhombuses, and dots mark the longitudinal axes of main areas of occurrence from WS climatologies at 310, 320, 330, and 340 K isentropic levels, respectively.

and 340 K) were plotted using different symbols to indicate the longitudinal axes of main COL occurrence from the WS climatology. It should be noted that the plot accounts only for areas of occurrence without representing the actual frequency of COLs. Such fields have been shown before in Figures 12, 13 and 18, 19. The very large differences in counts between these two approaches (almost an order of magnitude) is not from the actual number of individual COLs but results from the different approaches used in counting them. ERANAL and NCEPNAL (Figs. 12 and 13) represent a COL by a limited number of grid points that satisfy the four restrictive criteria imposed by the conceptual

model, whereas the WS methodology attributes the same COL event to many more grid points surrounded by a PV line. In a typical event, therefore, we have only one or two grid points indicating a COL when applying the ERANAL and NCEPNAL methods, but we can easily obtain 10 or more grid points using WS.

Further comparison between areas of occurrence (Fig. 20) shows that the higher the latitude of the COL region, the lower the isentropic level that is appropriate for the comparison. In the Asian and North American Atlantic sectors, the main areas of COLs were commonly detected at 310 and 320 K, while in the European and the North American Pacific areas,

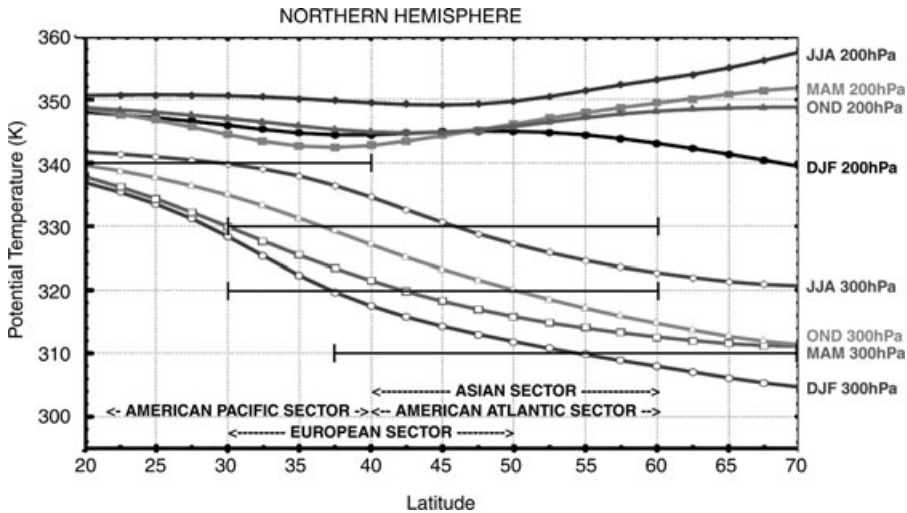


**Figure 21.** Mean seasonal potential temperature (K) corresponding to geopotential fields at 200 and 300 hPa for the extratropical Northern Hemisphere derived from NCAR-NCEP reanalysis. Main areas of COL occurrence are plotted over the latitude axis. Continuous black segments indicate the isentropic level where COLs are identified for different latitudes.

COLs were detected using 330 and 340 K. This applies for all seasons with the exception of winter when COLs occurring at higher latitudes were identified on lower isentropes. So, during winter, COLs in the European and North American Pacific areas were detected at 310, 320, and 330 K. In summary, for each season and for different areas of COL occurrence, different isentropic levels must be used to obtain a good representation of the main areas of COL occurrence. Given that we used two levels (200 hPa and 300 hPa) to detect ERANAL and NCEPNAL, the possible potential temperature intervals, as shown in Figure 21, were those between 310 and 350 K, depending on the different areas of occurrence and on the season. In general, the most appropriated isentropic levels to analyze each latitude band are: from 30°N to 60°N, 320 and 330 K; for latitudes lower than 40°N, 340 K; and for latitudes higher than 40°N, 310 K. Analysis of the seasonal cycle allows the comparison of the two approaches for COL identification. Most previous studies of COLs in the Northern Hemisphere agree that they are more frequent during the warm season, which is consistent with the relationship between COL development and

the strength and meander of the jet stream. Figure 22 shows the seasonal distribution of COLs for the three climatologies described in this paper, using several isentropic levels for the WS climatology (310, 320, 330, 340, and 350 K). In this comparison, we use only one COL point to represent each hourly cut-off low (and not all the points that fit the conditions imposed by the methods). The well-known seasonal pattern (maximum during summer and minimum during winter) is shown in all the analyzed climatologies, with some slight differences in the amplitude of the seasonal cycle. The best agreement is obtained between ERANAL, NCEPNAL, and WS for the 320 K level. Of all the seasons, the best agreement occurs in winter and the worst in summer when higher relative differences are found between the two approaches. The agreement between the seasonal cycles is also present in the monthly distribution of occurrence (Fig. 23), with a common maximum in July and common minima in December or January, and with a higher amplitude of the monthly cycle for the 340-K level than for the other climatologies.

The study reported herein reviews and expands previous multidecadal climatologies of

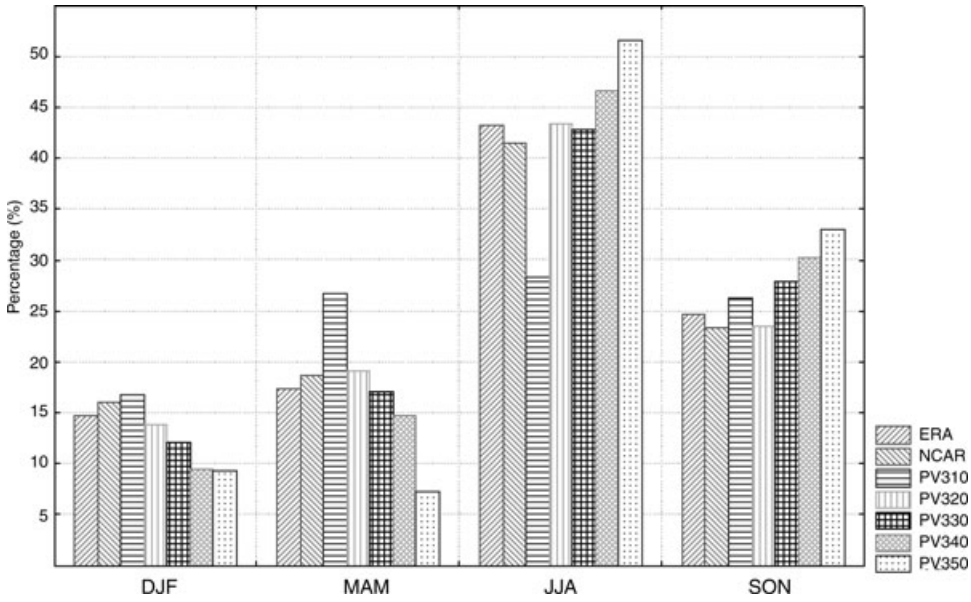


**Figure 22.** Seasonal distribution of the number of COL points for the three climatologies (five isentropes levels for WS, 310, 320, 330, 340, and 350 K).

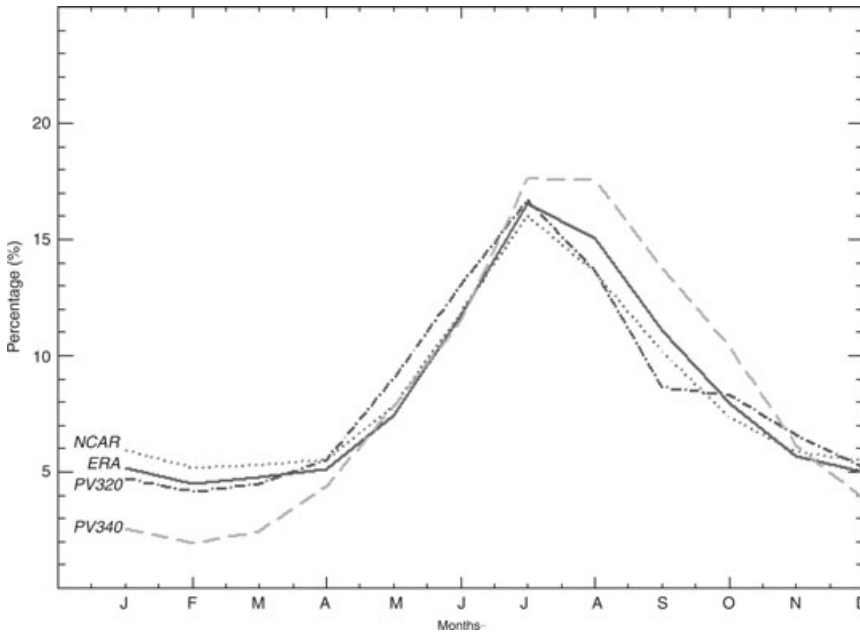


**Figure 23.** Monthly distribution of the number of COL points for the three climatologies (two isentropes levels for WS, 320, and 340 K).

cut-off low systems in the Northern Hemisphere. Cut-off lows were identified from data taken from the NCEP–NCAR and ERA-40 re-analyses, and the study makes use of two objective methods, one based on imposing the four main physical characteristics of the conceptual

model of cut-off lows and the other based on an analysis of IPV. The application of the algorithms to the extended data sets improves our ability to perform more accurate studies of the seasonal and interannual variability of these systems. Comparison between the results

derived from the two approaches shows that, in general terms, the agreement between the methods is good for extratropical areas. Apparent differences in the percentage time for which a grid point is part of a cut off is only a result of the particular method for counting the grid points that form a COL. For the COL data sets based on the conceptual model, the number of COL points detected is one order of magnitude lower than for the COL data set based on PV. The same COL could be represented by only a few very significant grid points for the approach based on the conceptual model or by many points for approaches based on PV, as the PV approach accounts for an area surrounded by a PV contour. That there is a different counting methodology does not have an influence on the main aspects of the climatology, such as the geographical distribution of COLs and their seasonal and monthly variability. In summary, the comparison between the climatologies reinforces the view that the conceptual model is well represented by the objective analysis technique developed by Nieto *et al.*<sup>26</sup> and that the climatology based on IPV analysis by Wernli and Sprenger<sup>6</sup> is in fairly close agreement. The two methodologies are complementary and each contributes to a better characterization of the physical properties of COLs.

### Acknowledgments

This work was supported by the Spanish Ministry of Education and Science under Grant CGL2007-65891-C05-01. R.N. acknowledges the Portuguese Ministry of Science through the Grant SFRH/BPD/22178/2005 by the FCT. The authors thank the anonymous reviewer for the helpful comments and suggestions. M. S. and H. W. thank MeteoSwiss for providing access to the ECMWF reanalysis data.

### Conflicts of Interest

The authors declare no conflicts of interest.

### References

1. Palmén, E. & C.W. Newton. 1969. *Atmospheric Circulation Systems: Their Structure and Physical Interpretation*. Academic Press. New York. 603 pp.
2. Winkler, R. & V. Zwatz-Meise. 2001. Manual of synoptic satellite meteorology. Conceptual models, Vers. 6.0. (Available at Central Institute for Meteorology and Geodynamics, Hohe Warte 38, 1190 Vienna, Austria).
3. Gimeno, L., R.M. Trigo, P. Ribera & J.A. García. 2007. Editorial: special issue on cut-off low systems (COL). *Meteorol. Atmos. Phys.* **96**: 1–2 (doi:10.1007/s00703-006-0216-5).
4. Kurz, M. 1998. *Synoptic Meteorology*. Deutscher Wetterdienst, Offenbach am Main, Germany 200 pp.
5. Hoskins, B.J., M.E. McIntire & A.W. Robertson. 1985. On the use and significance of isentropic potential vorticity maps. *Q. J. R. Meteor. Soc.* **111**: 877–946.
6. Wernli, H. & M. Sprenger. 2007. Identification and ERA-15 climatology of potential vorticity streamers and cutoffs near the extratropical tropopause. *J. Atmos. Sci.* **64**: 1569–1586.
7. Schwierz, C., S. Dirren & H.C. Davies. 2004. Forced waves on a zonally aligned jet stream. *J. Atmos. Sci.* **61**: 73–87.
8. Appenzeller, C., H.C. Davies & W.A. Norton. 1996. Fragmentation of stratospheric intrusions. *J. Geophys. Res.* **101**: 1435–1456.
9. Bamber, D.J., P.G.W. Healey, B.M.R. Jones, *et al.* 1984. Vertical profiles of tropospheric gases: chemical consequences of stratospheric intrusions. *Atmos. Environ.* **18**: 1759–1766.
10. Holton, J., P. Haynes, M. McIntyre, *et al.* 1995. Stratosphere–troposphere exchange. *Rev. Geophys.* **33**: 403–439.
11. Sprenger, M., H. Wernli & M. Bourqui. 2007. Stratosphere–troposphere exchange and its relation to potential vorticity streamers and cutoffs near the extratropical tropopause. *J. Atmos. Sci.* **64**: 1587–1602 (doi:10.1175/JAS3911.1).
12. Oltmans, S.J., H. Levy II, J.M. Harris, *et al.* 1996. Summer and spring ozone profiles over the North Atlantic from ozonesonde measurements. *J. Geophys. Res.* **101**: 29179–29200.
13. Gimeno, L., E. Hernández, A. Rúa & R. García. 1998. Surface ozone in Spain. *Chemosphere* **38**: 3061–3074.
14. Cuevas, E. & J. Rodríguez. 2002. Statistics of cut-off lows over the North Atlantic (in Spanish). Proc. Third Asamblea Hispano- Portuguesa de Geodesia y Geofísica, Comision Española de Geodesia y Geofísica, Valencia, Spain, pp. 1–3.
15. Kentarchos, A.S., G.J. Roelofs, J. Lelieveld & E. Cuevas. 2000. On the origin of elevated surface ozone

- concentrations at Izaña Observatory during the last days of March 1996: a model study. *Geophys. Res. Lett.* **27**: 3699–3702.
16. Wirth, V. 1995. Diabatic heating in an axisymmetric cutoff cyclone and related stratosphere–troposphere exchange. *Quart. J. Roy. Meteor. Soc.* **121**: 127–147.
  17. Wirth, V. & J. Egger. 1999. Diagnosing extratropical synoptic-scale stratosphere–troposphere exchange: a case study. *Quart. J. Roy. Meteor. Soc.* **125**: 635–656.
  18. Price, J.D. & G. Vaughan. 1993. The potential for stratosphere–troposphere exchange in cut-off low systems. *Quart. J. Roy. Meteor. Soc.* **119**: 343–365.
  19. Bourqui, M.S. 2006. Stratosphere–troposphere exchange from the Lagrangian perspective: a case study and method sensitivities. *Atmos. Chem. Phys.* **6**: 2651–2670.
  20. Gouget, H., G. Vaughan, A. Marenco & H.G.J. Smit. 2000. Decay of a cut-off low and contribution to stratospheretroposphere exchange. *Quart. J. Roy. Meteor. Soc.* **126**: 1117–1141.
  21. Knippertz, P. & J.E. Martin. 2005. Tropical plumes and extreme precipitation in subtropical and tropical West Africa. *Quart. J. Roy. Meteor. Soc.* **131**: 2337–2365.
  22. García-Herrera, R., D.G. Puyol, E.H. Martín, et al. 2001. Influence of the North Atlantic Oscillation on the Canary Islands precipitation. *J. Climate* **14**: 3889–3903.
  23. Tripoli, G.J., C.M. Medaglia, S.M. Dietrich, et al. 2005. The 9–10 November 2001 Algerian flood: a numerical study. *Bull. Amer. Meteor. Soc.* **86**: 1229–1235.
  24. Kotroni, V., K. Lagouvardos, E. Defer, et al. 2006. The Antalya 5 December 2002 storm: observations and model analysis. *J. Appl. Meteor. Clim.* **45**: 576–590.
  25. Porcú, F., A. Carrassi, C.M. Medaglia, et al. 2007. A study on cut-off low vertical structure and precipitation in the Mediterranean region. *Meteorol. Atmos. Phys.* **96**: 121–140 (doi:10.1007/s00703-006-0224-5).
  26. Nieto, R., L. Gimeno, L. de la Torre, et al. 2005. Climatologies features of cut-off low systems in the Northern Hemisphere. *J. Climate* **18**: 3085–3103.
  27. Matsumoto, S.K., K. Ninomiya, R. Hasegawa & Y. Miki. 1982. The structure and role of a subsynoptic cold vortex on the heavy precipitation. *J. Meteor. Soc. Japan* **60**: 339–353.
  28. Hill, E.F. & K.A. Browning. 1987. Case study of a persistent mesoscale cold pool. *Meteor. Mag.* **116**: 297–309.
  29. Keyser, D. & M.A. Shapiro. 1986. A review of the structure and dynamics of upper level frontal zones. *Mon. Wea. Rev.* **114**: 452–499.
  30. Delgado, G., A. Redaño, J. Lorente, et al. 2007. Cloud cover analysis associated to cut-off low pressure systems over Europe using Meteosat imagery. *Meteorol. Atmos. Phys.* **96**: 141–157 (doi:10.1007/s00703-006-0225-4. 2007).
  31. Huber-Pock, F. & C. Kress. 1981. Contributions to the problem of numerical frontal analysis. Proceedings of the Symposium on Current Problems of Weather-Prediction. Vienna, June 23–26, 1981. Publications of the Zentralanstalt für Meteorologie und Geodynamik, p. 253.
  32. Huber-Pock, F. & C. Kress. 1989. An operational model of objective frontal analysis based on ECMWF products. *Meteorol. Atmos. Phys.* **40**: 170–180.
  33. Sabo, P. 1992. Application of the thermal front parameter to baroclinic zones around cutoff lows. *Meteorol. Atmos. Phys.* **47**: 107–115.
  34. Renard, R.J. & L.C. Clarke. 1965. Experiments in numerical objective frontal analysis. *Mon. Wea. Rev.* **93**: 547–556.
  35. Zwatz-Meise, V. & F. Hufnagl. 1990. Some results about the relation between an objective front parameter and cloud bands in satellite images and its connection to classical cold front models. *Meteorol. Atmos. Phys.* **42**: 77–89.
  36. Nieto, R., L. Gimeno, J.A. Añel, et al. 2007. Analysis of the precipitation and cloudiness associated with COLs occurrence in the Iberian Peninsula. *Meteorol. Atmos. Phys.* **96**: 103–119 (doi:10.1007/s00703-006-0223-6).
  37. Jansá, A., A. Genoves & J.A. García-Moya. 2000. Western Mediterranean cyclones and heavy rain. Part I: numerical experiment concerning the Piedmont flood case. *Met. Apps.* **7**: 323–333.
  38. Hewson, T.D. 1998. Objective fronts Meteorol. *Appl.* **5**: 37–65.
  39. Ebel, A., H. Hass, H.J. Jakobs, et al. 1991. Simulation of ozone intrusion caused by tropopause fold and COL. *Atmos. Environ.* **25A**: 2131–2144.
  40. Langford, A., C. Masters, M. Proffitt, et al. 1996. Ozone measurements in a tropopause fold associated with a cut-off low system. *Geophys. Res. Lett.* **23**: 2501–2504 (and correction in Geophys Res Lett 24: 109–110).
  41. Qi, L., Y. Wang & L.M. Leslie. 2000. Numerical simulations of a cut-off low over southern Australia. *Meteorol. Atmos. Phys.* **74**: 103–115.
  42. Qi, L. & L.M. Leslie. 2001. Cut-off low pressure systems over southern Australia: a numerical modeling study and sensitivity experiments. *Aust. Meteor. Mag.* **50**: 183–194.
  43. Buckley, L., M. Leslie, W. Sullivan, et al. 2007. A rare East Indian Ocean autumn season tropical cut-off low: impacts and a high-resolution modelling study. *Meteorol. Atmos. Phys.* **96**: 61–84 (doi:10.1007/s00703-006-0221-8).

44. Ancellet, G., M. Beekmann & A. Papayannis. 1994. Impact of a cut-off lows development transport of ozone in the free troposphere. *J. Geophys. Res.* **99**: 3451–3468.
45. Barsby, J. & R.D. Diab. 1995. Total ozone and synoptic weather relationships over southern Africa and surrounding oceans. *J. Geophys. Res.* **100**: 3023–3032.
46. Kentarchos, A.S., T.D. Davies & C.S.A. Zerefos. 1998. Low latitude stratospheric intrusion associated with a cut-off low. *Geophys. Res. Lett.* **25**: 67–70.
47. Kentarchos, A.S., G.R. Roelofs & J. Lelieveld. 1999. Model study of a stratospheric intrusion event at lower midlatitude associated with the development of a cut-off low. *J. Geophys. Res.* **104**: 1717–1727.
48. Baray, J.L., S. Baldy, R.D. Diab & J.P. Cammas. 2003. Dynamical study of a tropical cut-off low over South Africa and its impact on tropospheric ozone. *Atmos. Environ.* **37**: 1475–1488.
49. Ravetta, F. & G. Ancellet. 2000. Identification of dynamical processes at the tropopause during the decay of a cut-off low using high resolution airborne lidar ozone measurements. *Mon. Wea. Rev.* **128**: 3252–3267.
50. Griffiths, M., M.J. Reeder, D.J. Low & Ra. A. Vincent. 1998. Observation of a cut-off low over southern Australia. *Quart. J. Roy. Meteor. Soc.* **124**: 1109–1132.
51. Price, J.D. & G. Vaughan. 1992. Statistical studies of cutoff-low systems. *Ann. Geophys.* **10**: 96–102.
52. Kentarchos, A.S. & T.D. Davies. 1998. A climatology of cutoff lows at 200 hPa in the Northern Hemisphere, 1990–1994. *Int. J. Climatol.* **18**: 379–390.
53. Parker, S.S., J.T. Hawes, S.J. Colucci & B.P. Hayden. 1989. Climatology of 500 mb cyclones and anticyclones 1950–85. *Mon. Wea. Rev.* **117**: 558–570.
54. Bell, G.D. & L.F. Bosart. 1989. A 15-year climatology of Northern Hemisphere 500 mb closed cyclone and anticyclone centers. *Mon. Wea. Rev.* **117**: 2142–2163.
55. Novak, M.J., L.F. Bosart, D. Keyser, *et al.* 2002. Climatology of warm season 500 hPa cutoff cyclones and a case study diagnosis of 14–17 July 2000. Preprints, 19th Conf. on Weather Analysis and Forecasting, Amer. Meteor. Soc., San Antonio, TX, pp. 68–71.
56. Hernández, A. 1999. Un Estudio Estadístico sobre Depresiones Aisladas en Niveles Altos (DANAs) en el Sudoeste de Europa basado en Mapas Isentrópicos de Vorticidad Potencial. IV Simposio Nacional de Predicción, Instituto Nacional de Meteorología, Serie Monogr., No. SM 351, Ministerio de Medio Ambiente, 235 pp.
57. Qi, L., L.M. Leslie & S.X. Zhao. 1999. Cut-off low pressure systems over southern Australia: climatology and case study. *Int. J. Climatol.* **19**: 1633–1649.
58. Smith, B.A., L.F. Bosart, D. Keyser & D. St. Jean. 2002. A global 500hPa cutoff cyclone climatology: 1953–1999. Preprints, 19th Conf. on Weather Analysis and Forecasting, Amer. Meteor. Soc., San Antonio, TX, pp. 1–14.
59. Kalnay, E. *et al.* 1996. The NCEP/NCAR 40-Year Reanalysis Project. *Bull. Amer. Meteor. Soc.* **77**: 437–471.
60. Uppala, S., P. Kallberg, A. Hernández, *et al.* 2004. ERA-40: ECMWF 45-year reanalysis of the global atmosphere and surface conditions 1957–2002. *ECMWF Newsletter* **101**: 2–21.
61. Fuenzalida, H.A., R. Sánchez & R.D. Garreaud. 2005. A climatology of cutoff lows in the Southern Hemisphere. *J. Geophys. Res.* **110**: D18101 (doi:10.1029/2005JD005934).
62. Pizarro, J. & A. Montecinos. 2000. Cut-off cyclones off the subtropical coast of Chile. Preprints 6th Int. Conf. on Southern Hemisphere Meteorology and Oceanography, pp 278–279.
63. Campetella, C.M. & N.E. Possia. 2007. Upper-level cut-off lows in southern South America. *Meteorol. Atmos. Phys.* **96**: 181–191 (doi:10.1007/s00703-006-0227-2).
64. Nieto, R., L. Gimeno, L. de la Torre, *et al.* 2007. Interannual variability of cut-off low systems over the European sector: The role of blocking and the Northern Hemisphere circulation modes. *Meteorol. Atmos. Phys.* **96**: 85–101 (doi:10.1007/s00703-006-0222-7).
65. Croci-Maspoli, M., C. Schwiertz & H.C. Davies. 2007. A multifaceted climatology of atmospheric blocking and its recent linear trend. *J. Climate* **20**: 633–649.
66. Koch, P., H. Wernli & H.C. Davies. 2003. An event-based jet-stream climatology and typology. *Int. J. Climatol.* **26**: 283–301.
67. Hurrell, J.W. 1995. Decadal trends in the North Atlantic Oscillation: regional temperatures and precipitation. *Science* **269**: 676–679.
68. Trenberth, K.E., G.W. Branstator, D. Karoly, *et al.* 1998. Progress during TOGA in understanding and modelling global teleconnections associated with tropical sea surface temperatures. *J. Geophys. Res.* **103**(C7): 14291–14324.
69. Waugh, D.W. & P.P. Rong. 2002. Interannual variability in the decay of lower stratospheric arctic vortices. *J. Meteor. Soc. Japan.* **80**: 997–1012.
70. Black, R.X., B.A. McDaniel & W.A. Robinson. 2006. Stratosphere-troposphere coupling during spring onset. *J. Climate* **19**: 4891–4901.
71. Wernli, H. & H.C. Davies. 1997. A Lagrangian-based analysis of extratropical. I: The method and some applications. *Quart. J. Roy. Meteor. Soc.* **123**: 467–489.